Cell Reports

Article

Precision off-the-shelf natural killer cell therapies for oncology with logic-gated gene circuits

Graphical abstract

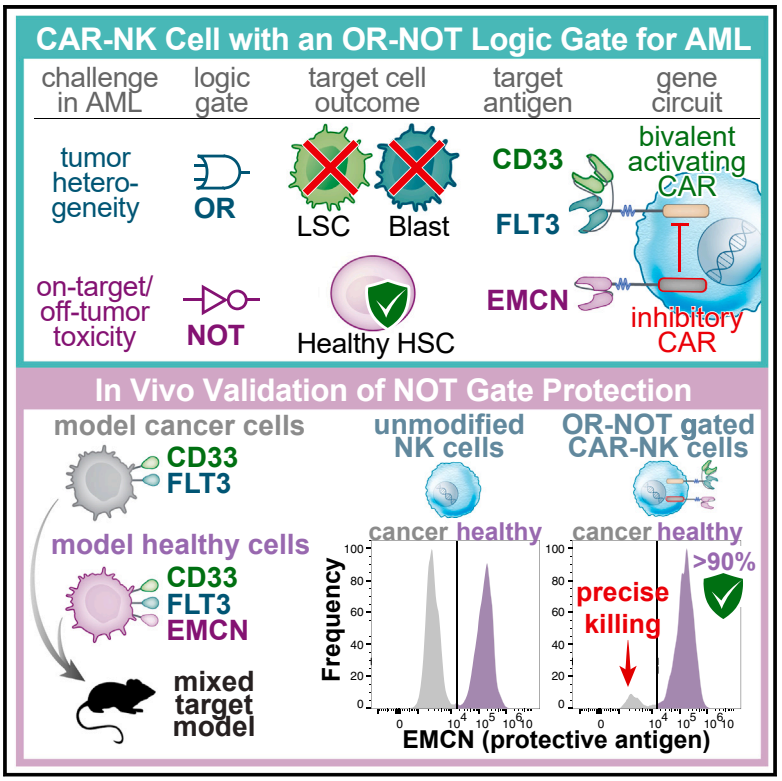

Highlights

- A three-input logic gate with activating and inhibitory CARs is optimized in NK cells
- Logic-gated NK cells kill leukemic stem cells and blasts, not healthy stem cells
- Selective killing of tumor cells is validated *in vivo* in a mixed target cell model

Authors

Nicholas W. Frankel, Han Deng, Gozde Yucel, ..., Russell Gordley, Timothy K. Lu, Brian S. Garrison

Correspondence

nicholas.frankel@sentibio.com (N.W.F.), tim.lu@sentibio.com (T.K.L.), brian.garrison@sentibio.com (B.S.G.)

In brief

Treating acute myeloid leukemia with conventional, single-target CAR cell therapies is challenging due to tumor heterogeneity and because tumor antigens are found on hematopoietic stem cells. Frankel et al. design logic-gated CAR-natural killer cells that simultaneously detect three antigens on prospective target cells to safely decide whether to kill them.

Frankel et al., 2024, Cell Reports *43*, 114145
May 28, 2024
https://doi.org/10.1016/j.celrep.2024.114145

CellPress

Cell Reports

CellPress
OPEN ACCESS

Article

Precision off-the-shelf natural killer cell therapies for oncology with logic-gated gene circuits

Nicholas W. Frankel,[1,4,*] Han Deng,[1,4] Gozde Yucel,[1] Marcus Gainer,[1] Nelia Leemans,[1] Alice Lam,[1] Yongshuai Li,[1] Michelle Hung,[1] Derrick Lee,[1] Chen-Ting Lee,[1] Andrew Banicki,[1] Mengxi Tian,[1] Niran Almudhfar,[1] Lawrence Naitmazi,[1] Assen Roguev,[1] Seunghee Lee,[2] Wilson Wong,[2] Russell Gordley,[1] Timothy K. Lu,[1,3,*] and Brian S. Garrison[1,5,*]

[1]Senti Biosciences, Inc., South San Francisco, CA 94080, USA
[2]Boston University, Boston, MA 02215, USA
[3]Massachusetts Institute of Technology, Cambridge, MA 02139, USA
[4]These authors contributed equally
[5]Lead contact
*Correspondence: nicholas.frankel@sentibio.com (N.W.F.), tim.lu@sentibio.com (T.K.L.), brian.garrison@sentibio.com (B.S.G.)
https://doi.org/10.1016/j.celrep.2024.114145

SUMMARY

Acute myeloid leukemia (AML) is an aggressive disease with a poor prognosis (5-year survival rate of 30.5% in the United States). Designing cell therapies to target AML is challenging because no single tumor-associated antigen (TAA) is highly expressed on all cancer subpopulations. Furthermore, TAAs are also expressed on healthy cells, leading to toxicity risk. To address these targeting challenges, we engineer natural killer (NK) cells with a multi-input gene circuit consisting of chimeric antigen receptors (CARs) controlled by OR and NOT logic gates. The OR gate kills a range of AML cells from leukemic stem cells to blasts using a bivalent CAR targeting FLT3 and/or CD33. The NOT gate protects healthy hematopoietic stem cells (HSCs) using an inhibitory CAR targeting endomucin, a protective antigen unique to healthy HSCs. NK cells with the combined OR-NOT gene circuit kill multiple AML subtypes and protect primary HSCs, and the circuit also works *in vivo*.

INTRODUCTION

Chimeric antigen receptors (CARs) are synthetic transmembrane receptors that recognize tumor-associated antigens (TAAs) on a target cell surface and redirect the cytotoxic capabilities of immune cells such as T cells or natural killer (NK) cells against these cells. CAR-T and CAR-NK products have shown promise as cancer therapies for select blood cancers and are being clinically investigated for a wide variety of liquid and solid tumor indications. NK cells present several possible advantages over T cells, including their innate anti-tumor activities, reduced propensity to cause systemic toxicity, and low alloreactivity, which may facilitate the manufacture of lower-cost, off-the-shelf products.[1]

Existing single-target modalities, such as antibodies, antibody-drug conjugates, and conventional CAR-based cell therapies, rely on a single TAA to distinguish between cancer and healthy cells. When such TAAs are also found on normal tissues, however, there is a risk of on-target/off-tumor toxicity that fundamentally limits the therapeutic window between efficacy and safety.[2] As a result, many cancers that lack a single "clean" TAA, such as AML, still constitute a major untreated disease burden.

AML is an acute leukemia characterized by an accumulation of malignant immature white blood cells due to differentiation blockade. It is the most common type of acute leukemia in adults, constituting 80%–85% of cases,[3,4] and is the second most common—as well as the deadliest—in children.[5] Conventional therapy consists of remission induction therapy followed by consolidation, in which multiple courses or high doses of chemotherapy are followed by hematopoietic stem cell (HSC) transplantation.[6] Even so, ~70% of patients relapse within 3 years.[7,8]

Unfortunately, the successes of CAR-based cell therapies have not yet been translated to treatment of AML, likely due to the lack of a single suitable lineage-restricted TAA that is: (1) expressed on both AML blast and leukemic stem cell (LSC) populations; and (2) not expressed on healthy cells, such as HSCs (refer to Table S4 for immunophenotypes of these cellular subpopulations). CD33 (SIGLEC-3) and FLT3 (CD135) are validated therapeutic targets for AML. CD33 is a myeloid differentiation marker[9] expressed on AML and currently targeted in the clinic using the Food and Drug Administration (FDA)-approved drug, gemtuzumab ozogamicin (Mylotarg).[10] FLT3 is a potential CAR target for AML blasts and LSCs,[11–14] which is promising because recent studies suggest that AML relapse is associated in part with the LSC population.

Targeting LSCs has been challenging, however, due to the risk of on-target/off-tumor toxicity.[11] For example, while FLT3 is a promising CAR target for AML, FLT3 CAR cell therapies have

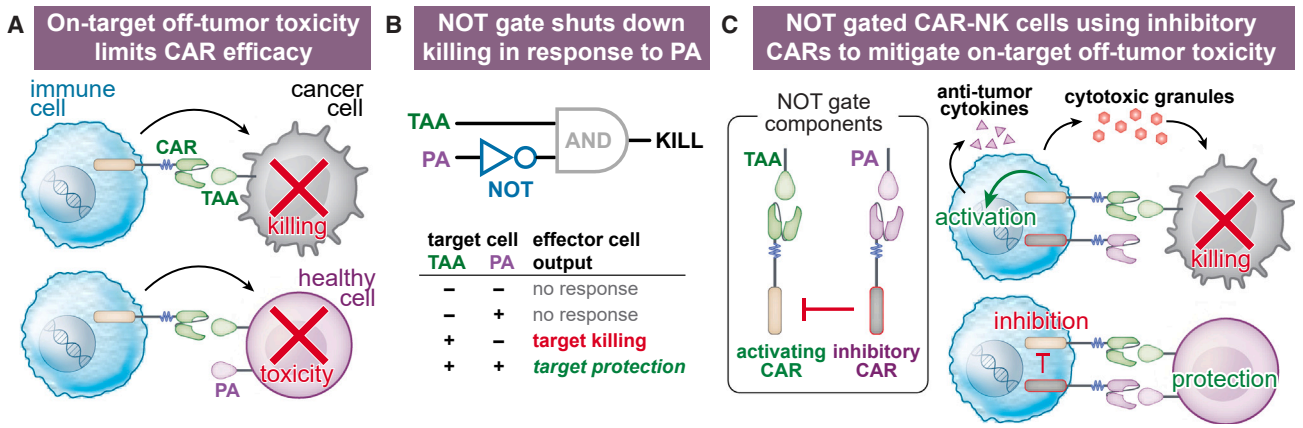

Figure 1. NOT gates based on inhibitory CARs can be used to make CAR-NK cells with enhanced precision and wider therapeutic windows

(A) Therapeutic immune cells with activating CARs (aCARs) targeting tumor-associated antigens (TAAs) can kill healthy cells that express the TAA (on-target/off-tumor toxicity). We have discovered cell-surface proteins that are selectively expressed on healthy cells, not but cancer cells, that can be recognized as protective antigens (PAs).

(B) NOT gates invert signals, allowing detection of a PA to shut down TAA-targeted killing of healthy cells.

(C) We implemented NOT gates in NK cells by designing inhibitory CARs (iCARs) that recognize PAs and shut down aCAR-triggered killing in response to TAAs, sparing healthy cells.

remained unavailable in the United States and Europe due to concerns over toxicity against healthy FLT3$^+$ HSCs and early progenitors cells (HSPCs),[15,16] as has already been observed in FLT3 CAR-T cell and bispecific T cell engager preclinical studies.[17–20] While B cell aplasia that results from anti-CD19 CAR-T therapy can be clinically managed with immunoglobulin replacement therapy,[21] anti-AML T cell-based therapies with off-tumor toxicity toward healthy HSPC populations have the potential to cause significant and life-threatening treatment complications, including anemia, thrombocytopenia, or even bone marrow failure.[22] Therefore, safe and effective cell therapies for AML will require tools to shield healthy cells from the deleterious effects of anti-AML CARs and must target both AML blasts and LSCs despite the fact they often have different TAAs.

The lack of clean TAAs could be overcome if therapeutic modalities could instead detect multiple antigens and control cytotoxic activity based on which combination of antigens are absent or present. To measure cancer-specific signatures[23] rather than just individual TAAs, we designed CAR-based logic gates in NK cells that detect and respond to multiple inputs. Specifically, we created OR logic-gated CARs to target multiple tumor subpopulations and to mitigate the risk of TAA expression loss.[24,25] Furthermore, we designed a NOT logic gate to enable CAR-NK cells to detect the presence of a protective antigen (PA) on the surface of healthy cells and thus protect them from being killed due to on-target/off-tumor expression of dirty TAAs.

We validated these logic gates individually and in concert, both *in vitro* and *in vivo*, and confirmed the ability of OR-NOT gate CAR-NK cells to target TAAs of multiple AML subpopulations while sparing primary healthy human HSCs from on-target/off-tumor toxicity. This implementation of OR-NOT logic gating in CAR-NK cells against clinically relevant cancer antigens has the potential to enhance efficacy and precision for the treatment of AML and is being advanced toward first-in-class clinical trials in patients.

RESULTS

Most TAAs are not restricted solely to cancer cells, so T or NK cells expressing a TAA-specific CAR may recognize and kill TAA-expressing healthy cells (Figure 1A). A protective mechanism is needed to prevent this on-target/off-tumor toxicity and thus maximize treatment efficacy and precision. NOT gates—components that invert signals—can be used to build circuits that shut down cellular activity in response to the presence of an "off" signal (Figure 1B). To create such a circuit in the context of CAR-NK cells, we designed an inhibitory CAR (iCAR) to recognize a PA on healthy target cells and inhibit activating CAR (aCAR)-mediated killing of those healthy cells (Figure 1C).

FLT3 is a clinically validated TAA in AML that is also expressed on healthy HSCs (Figure 2A). There are multiple FDA-approved small-molecule drugs that distinguish between FLT3$^+$ cancer cells and FLT3$^+$ healthy cells by targeting cancer-specific mutations in the FLT3 intracellular domain. Targeting FLT3 with antibody-based or CAR-based therapies has been challenging, however, because there are no such distinguishing mutations in the extracellular domain. Therefore, to distinguish these two cell types, we screened for "negative" targets marking healthy cells rather than conventional "positive" targets marking cancer cells (Figure 2B).

Understanding that a curative therapeutic approach for AML likely must target the LSC population in order to prevent relapse of disease in patients, our approach was to combine (1) an anti-FLT3 aCAR targeting AML with (2) an iCAR that detects and protects healthy HSCs, enhancing the therapeutic window. To identify PAs expressed by HSCs but not AML, we used a bioinformatics pipeline (Figure 2B) that filtered for membrane proteins, expression on HSCs, and low RNA counts on AML, which nominated several candidates which we then profiled by flow cytometry. Our manual curation process of the resulting hits

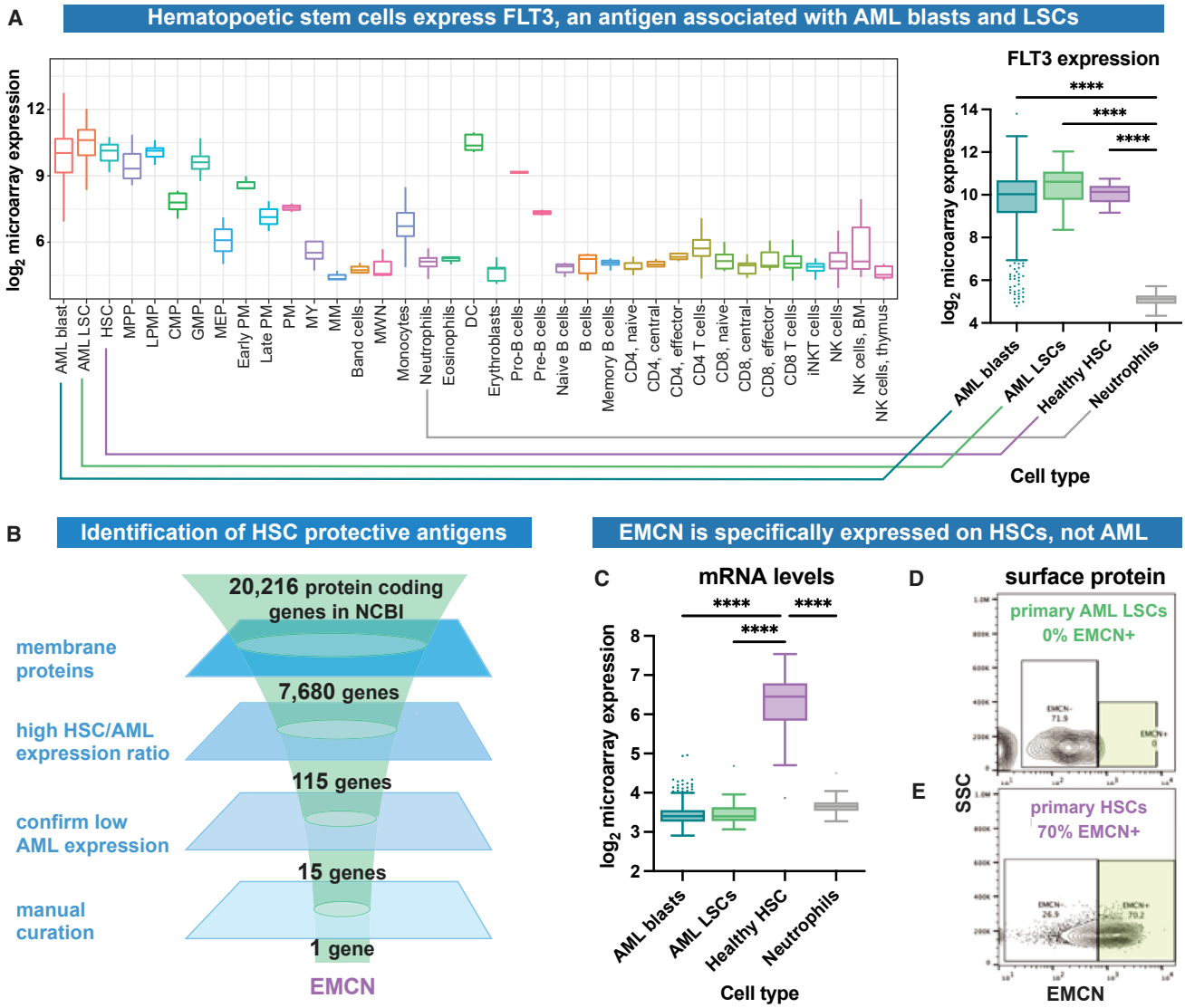

Figure 2. Discovery of EMCN as a PA for healthy HSCs during CAR-mediated therapy against AML

(A) FLT3 expression was compared between AML and healthy hematopoietic cell subpopulations (left; for additional subpopulation details, see Table S4), with focused comparative analysis between AML blasts ($n = 825$), AML patient LSCs ($n = 28$), and healthy donor HSCs ($n = 22$), with healthy donor neutrophils ($n = 2$) as a control (right).

(B) Bioinformatics pipeline summary for identifying HSC-specific PAs not expressed on AML.

(C) EMCN expression was compared between the same groups as (A, right), showing high expression in healthy HSCs compared to AML blasts or LSCs.

(D and E) EMCN protein expression was assayed by flow cytometry in patient-derived AML LSCs (D) and primary HSCs from healthy donors (E), validating selective expression of EMCN on HSCs. SSC, side scatter.

In this figure, box plots follow Tukey's convention, with outliers omitted from (A) for visual clarity. Statistical significance determined using ANOVA (****$p < 0.001$).

consisted of consideration of the HSC literature, which narrowed our choice to endomucin (EMCN) (Figure 2C) due to the fact that it was previously demonstrated to be a marker that is robustly expressed on highly functional HSCs possessing long-term multi-lineage reconstitution potential.[26] We confirmed that the healthy HSC compartment in primary human bone marrow cells expressed EMCN at a frequency of up to 70%, while patient-derived AML LSC samples demonstrated no appreciable expression (Figures 2D vs. 2E).

Next, we designed an aCAR/iCAR receptor pair to kill FLT3$^+$ AML cells while protecting EMCN$^+$ healthy cells from CAR-mediated toxicity (Figure 3A, left). We created an FLT3 aCAR with a CD28-derived co-stimulatory domain and CD3z stimulatory domain (aFLT3-28z). Like the aCAR, the iCAR had extracellular antigen-recognition and hinge domains and a transmembrane domain. Unlike the aCAR's intracellular domains (ICDs), which are derived from T cell receptor signaling components with immunoreceptor tyrosine-based activation motifs (ITAMs), the

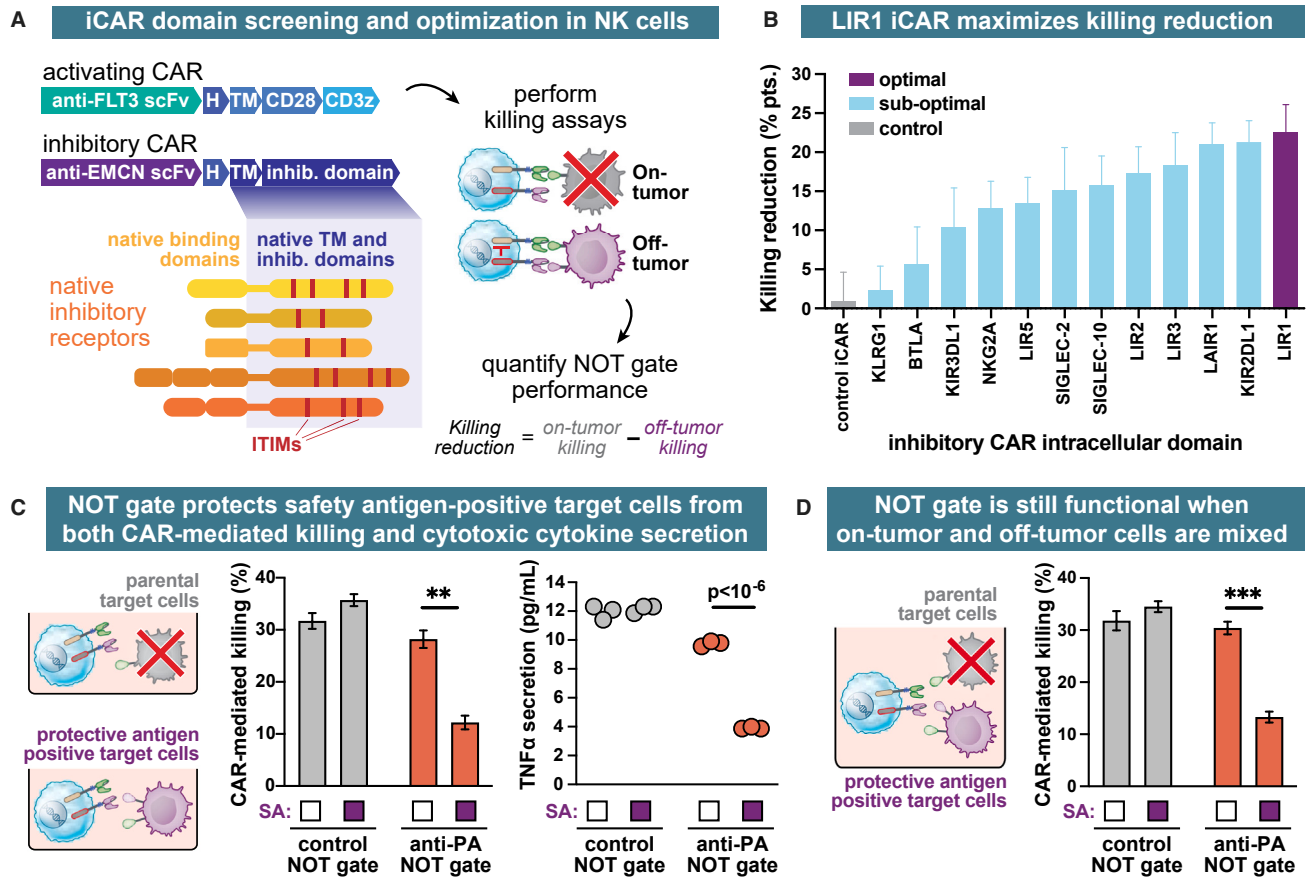

Figure 3. Design and optimization of "FLT3 NOT EMCN" logic gate in CAR-NK cells

(A) We developed a systematic approach to design the NOT gate by screening different transmembrane and intracellular domains (TM-ICDs) taken from native inhibitory proteins in the context of an anti-EMCN iCAR, which were co-transduced into NK cells with an aFLT3 aCAR. Constructs were evaluated based on the difference between on-tumor (FLT3$^+$EMCN$^-$) killing and off-tumor (FLT3$^+$EMCN$^+$) killing (or "killing reduction"). scFv, single-chain Fv (variable fragment); H, hinge; TM, transmembrane domain; ITIM, immunoreceptor tyrosine inhibitory motif.

(B) Comparison of NOT gates using aFLT3 aCAR combined with aEMCN iCARs with different TM-ICDs, demonstrating optimality of the LIR1-derived TM-ICD (purple) by its high killing reduction. Control: aFLT3 aCAR with LIR1-based iCAR targeting an irrelevant antigen.

(C) CAR-mediated killing (bars) and TNF-α secretion (circles) of NK cells in (B) in response to on- or off-tumor cells. Anti-PA NOT gate (aFLT3-28z and aEMCN-LIR1) significantly reduced aCAR response in a PA-dependent manner.

(D) Mixed target challenge. Same cell and antigen system as (C) except that both target cell types were mixed in the same container, showing the same level of protection.

In this figure, values represent the mean of three technical replicates, and error bars represent ±SE of mean. Welch's test was used to discern significant differences.

iCAR had ICDs adapted from immune checkpoint receptors with immunoreceptor tyrosine-based inhibitory motifs (ITIMs). This design takes advantage of the rapid, protein-based signaling of ITIMs, which recruit phosphatases SHP-1, SHP-2, and SHIP-1 to the immune synapse, blocking phosphorylation cascades arising from activated ITAMs on the intracellular tails of activating receptors (e.g., DAP12, CD3z, and FceRIg).[27] We packaged the aFLT3-28z and aEMCN iCAR constructs into viral vectors and co-transduced them into NK cells to create NOT gate CAR-NK cell populations. We also constructed a control NOT gate, which was targeted against a dummy antigen, HER2, not expressed on any target cells. Antibiotic selection for the iCAR construct was used to ensure that aCAR$^+$ NK cells were also iCAR$^+$ (Figure S2A).

NK cells expressing NOT gates with these various iCARs were then screened in parallel (Figure 3A, upper right) for their ability to kill "on-tumor" target cells (a leukemia cell line, SEM, endogenously expressing FLT3) while sparing "off-tumor" target cells (the same cell line engineered to express EMCN). We compared NOT gate performance by calculating the reduction in killing between on-tumor and off-tumor targets (Figure 3B, lower right). Higher killing reduction signified more potent inhibitory signaling by the iCAR intracellular domain.

The control NOT gate with a non-targeting binder (gray bars in Figures 3B and 3C) resulted in equal killing of on- and off-tumor cells, thereby exhibiting no killing reduction, signifying no NOT gate function. NOT gates with functional iCARs (Figure 3B, blue bars) had positive killing reduction (i.e., lower killing of

CellPress
OPEN ACCESS

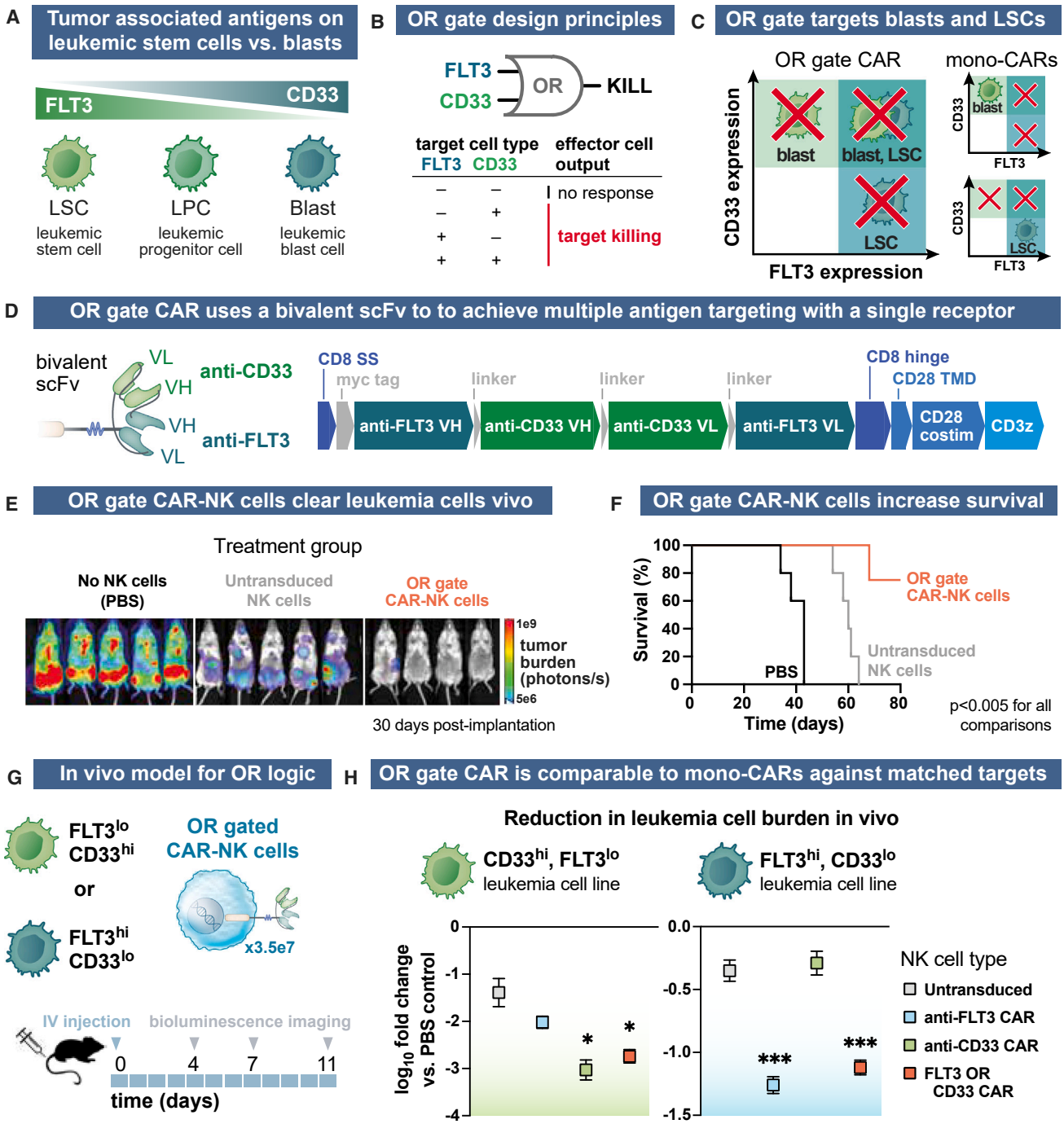

Figure 4. OR-gated CARs enable NK cells to target multiple AML antigens

(A) In AML, less-differentiated LSCs tend to express more FLT3, while more-differentiated blasts tend to express more CD33.

(B) OR gates are circuit components that activate in the presence of either or both inputs.

(C) CARs that target only FLT3 or only CD33 cannot target all AML blasts or LSCs, respectively, while OR gate CARs targeting both antigens may recognize multiple AML subpopulations.

(D) OR gate CAR structure based on loop bivalent scFv with both FLT3 and CD33 recognition domains. VH and VL, variable heavy and light domains.

(E) *In vivo* validation of OR gate CAR-NK cell killing in an endogenously FLT3^{+}CD33^{+} MV4-11 leukemia xenograft model expressing luciferase. Bioluminescence imaging shows CAR-mediated tumor clearance (right) in comparison with untransduced NK cells (middle). Left: PBS treatment control.

(legend continued on next page)

off-target than on-target cells), signifying varying levels of NOT gate function. The NOT gate using an iCAR derived from leukocyte immunoglobulin-like receptor subfamily B member 1, or LIR1 (Figure 3B, purple; Figures 3C and 3D, red) demonstrated the greatest level of killing reduction and therefore the highest level of NOT gate function.

The NOT gate based on the LIR1 iCAR showed minimal tonic inhibition of aCAR function in the absence of EMCN expression on targets relative to the control NOT gate (Figure 3C). Moreover, it was able to suppress the secretion of tumor necrosis factor α (TNF-α) (Figures 3C [right] and S3A) and interferon-γ (Figure S2C) in an EMCN-dependent fashion. The high performance of the LIR1 iCAR was not dictated by high expression level alone, as other iCARs with similar expression performed substantially worse (Figure S3B). Statistically significant EMCN-dependent suppression of toxicity was robust across multiple biological replicates (Figure S2D).

EMCN-dependent reduction in killing was also observed when $EMCN^+$ and $EMCN^-$ target cells were premixed and co-cultured with NOT gate CAR-NK cells with the aEMCN-LIR1 iCAR (Figures 3D and S2B). These data suggest that the "FLT3 NOT EMCN" circuit enables cell-by-cell decision making with no loss of function in a well-mixed environment, implying that the circuit works on a fast timescale, as would be expected from the ITIM-mediated mechanism of action based on protein recruitment and modification. This is particularly important for clinical applications in oncology, where healthy cells and cancer cells are often in close proximity to each other. For example, in AML, cancer cells intermingle continuously with healthy hematopoietic cells.

Since no single TAA can be used to wholly target all AML subpopulations, we developed a bioinformatics pipeline (Figure S4A) to identify target antigen pairs which together possess the potential to concurrently eliminate both LSCs and blasts. FLT3 is often more associated with less-differentiated hematopoietic cells, including LSCs, while CD33 is often more highly expressed within more-differentiated myeloid cells, including blasts,[28] and inconsistently expressed among LSCs[29] (Figure 4A). Concurrent targeting of both FLT3 and CD33 should: (1) produce an inclusive targeting approach covering all AML subpopulations; (2) help prevent tumor antigen escape; and (3) increase total killing of the many AML cells that are double positive for FLT3 and CD33 expression. Thus, this OR gate strategy, which activates when either of two inputs (or both) is detected (Figure 4B), should have advantages over conventional "mono-CARs" that only target one subpopulation (Figure 4C).

We created an "FLT3 OR CD33" circuit using a bivalent aCAR design containing two binders, one for CD33 and one for FLT3, combined in a loop configuration[25] (Figure 4D). As with the aFLT3 aCAR above, the intracellular domain of the OR gate CAR consisted of CD28 co-stimulatory and CD3z stimulatory domains. We tested *in vivo* efficacy of OR gate CAR-NK cells within an AML xenograft immunocompromised mouse model generated with patient-derived MV4-11 AML cells, which endogenously express FLT3 and CD33. Target and effector cells were both injected on day 0. This approach has been shown to be clinically translatable in the field of CAR-NK cell therapy, with results having been successfully translated from bench[30] to bedside[31,32] and back to bench, using the same approach again with patient samples.[33] Other preclinical studies[34,35] in the field have taken this approach as well.

Bioluminescence imaging (BLI) of tumor-expressed luciferase (Figures 4E and S4B) revealed the innate cytotoxic behavior of untransduced NK cells compared to a saline (PBS) control (middle vs. left groups), but OR gate CAR-NK cells exhibited substantially higher suppression of tumor burden than untransduced NK cells alone (right vs. middle group). As a result of the OR-gated CAR-mediated tumor killing, mouse survival was also significantly extended compared to the other treatment groups (Figure 4F).

After confirming the cytotoxic activity of the OR-gated CAR *in vivo*, we sought to verify its logic gating performance in comparison to mono-CARs that solely bind only FLT3 or CD33. We created an *in vivo* OR gate vs. mono-CAR challenge by injecting two different groups of immunocompromised mice with either SEM leukemia cells, which endogenously express high levels of FLT3 and low levels of CD33, or MOLM-13 leukemia cells, which endogenously express low levels of FLT3 and high levels of CD33. Both patient-derived cell lines expressed luciferase, allowing us to track tumor burden and progression, as well as CAR-NK cell anti-tumor activity compared to a PBS control (Figure 4G).

As expected, based on antigen expression levels, anti-FLT3 mono-CAR-NK cells statistically significantly reduced tumor burden in the $FLT3^{hi}$ SEM high tumor model but not in the $FLT3^{lo}$ MOLM-13 tumor model (Figure 4H, blue box in left vs. right plot; Figure S5). Anti-CD33 mono-CAR-NK cells, on the other hand, showed the expectedly reversed trend by specifically killing the $CD33^{hi}$ tumor model but not the $CD33^{lo}$ tumor model (Figure 4H, green box in left vs. right plot). Importantly, OR-gated CAR-NK cells with both FLT3 and CD33 binders reduced tumor burden in both models, to a similar extent as each mono-CAR in its own "specialized" tumor model (Figure 4H, red box in both left and right plots). Thus, the OR-gated CAR results in an increased breadth of targeting across different heterogeneous leukemia models with varying expression levels of AML antigens FLT3 and CD33.

We combined OR and NOT gate components to make a "(FLT3 OR CD33) NOT EMCN" circuit that targets both AML LSC and blast antigens while also protecting vulnerable

(F) Kaplan-Meier curve of mouse study in (E), showing survival extension with OR gate CAR-NK cell treatment (red) relative to other groups. All groups are significantly different from each other ($p < 0.005$, log-rank test, 4–5 mice per group).

(G) *In vivo* OR gate challenge: NK cells were injected into two groups of mice, each engrafted with either SEM cells (FLT3hi, CD33lo) or MOLM13 cells (FLT3lo, CD33hi).

(H) Change in tumor burden (measured by BLI) relative to PBS treatment control in each of the two challenge groups, comparing mono-CARs (blue, green) to the OR gate CAR (red; day 11 post injection). Mono-CARs each target one tumor type, while OR gate CAR (red) targets both. Markers represent mean of at least five mice; error bars represent ±SE of mean. Significant differences assessed with ANOVA (*$p < 0.05$, ***$p < 0.005$).

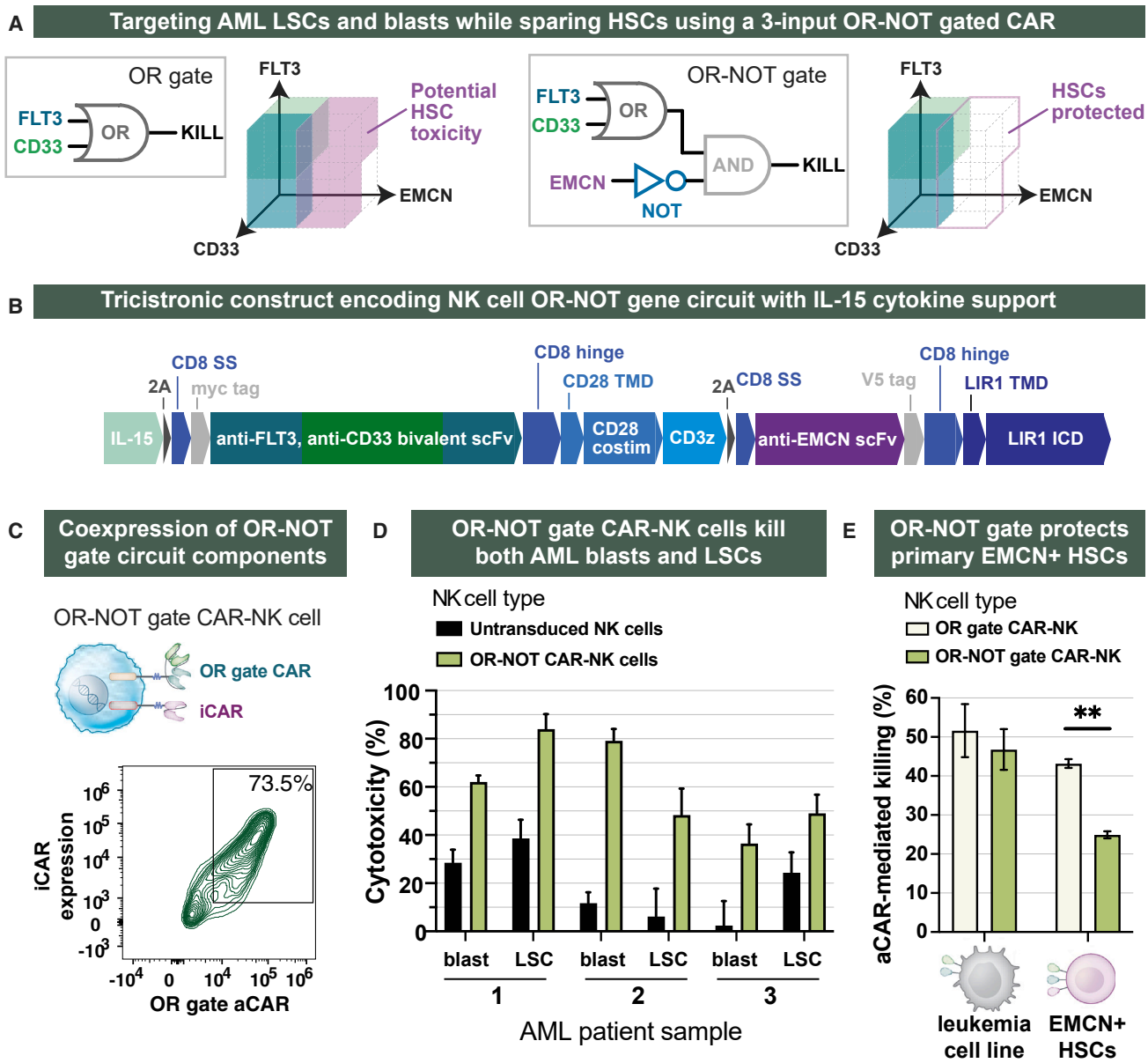

Figure 5. Combining OR and NOT gates to protect primary healthy human hematopoietic stem cells

(A) Applying NOT gate architecture to the OR-gated CAR yields an OR-NOT gate circuit that targets multiple AML subpopulations while protecting HSCs. Three-dimensional antigen space reveals how 3-input logic gating is required to achieve this clinical goal by targeting cells defined by specific combinations of the three antigens.

(B) Construct design incorporating OR gate aCAR, aEMCN iCAR, and a modified form of IL-15 (to enhance NK cell persistence) into a single tricistronic payload.

(C) OR gate aCAR and iCAR from construct design in (B) were co-expressed at high levels. Gate was set based on an untransduced NK cell control.

(D) Killing of blasts and LSCs from multiple AML patient samples by OR-NOT gate NK cells (green) is enhanced compared to untransduced NK cells (black).

(E) OR-NOT gate CAR-NK cells (medium green) reduce killing of EMCN$^+$ HSCs from freshly thawed primary human CD34-enriched bone marrow cells, compared to OR gate CAR-NK cells without the NOT gate (light green).

No statistically significant reduction of killing occurs in response to SEM leukemia cells. Values represent the mean of three technical replicates, and error bars represent ±SE of mean. Welch's test was used to discern significant differences (**$p < 0.01$).

EMCN$^+$ HSCs (Figure 5A). To do so, we designed a construct encoding an anti-FLT3/anti-CD33 bivalent aCAR, an anti-EMCN iCAR, and a modified form of interleukin-15 (IL-15), a cytokine that can enhance NK cell persistence,[36] all on a single tricistronic retroviral payload (Figure 5B), and confirmed high levels of aCAR and iCAR co-expression in NK cells (Figure 5C).

NK cells transduced with the tricistronic construct showed a majority of cells expressing all three payloads, demonstrating

the ability to express multiple logic gates in NK cells along with another clinically important effector (Figure 5C). OR-NOT gate CAR-NK cells showed enhanced killing of both AML blasts and LSCs from multiple patient samples (Figure 5D). Significant NOT gate performance was confirmed across a large number of NK cell donors (ten of ten tested, Figure S8A), highlighting the robustness of the gene circuit, even in the context of an aCAR targeting multiple AML antigens and co-expression of a clinically useful activator, IL-15. While we found that aCAR and iCAR responses did scale with antigen density on target cells, we confirmed that NOT gate function was robust across a range of TAA or PA expression levels. The EMCN iCAR maintains a comparable level of protection (20 to 25 percentage points of killing reduction) even when challenged with target cells with 10-fold lower FLT3 expression level (Figure S8B). While EMCN iCAR function does depend modestly on target EMCN expression levels, changing EMCN expression level on the target cells by 6-fold results in a change of protection by only 1.3-fold, signifying a relatively insensitive relationship (Figure S8C).

We have shown that the NOT gate protects target cells in a PA-dependent manner using an experimental system in which healthy cells are modeled by cell lines overexpressing the PA, but how well does the circuit perform in protecting actual primary EMCN$^+$ HSCs? We compared OR gate CAR-NK cells expressing the "FLT3 OR CD33" gene circuit to OR-NOT gate CAR-NK cells expressing the full "(FLT3 OR CD33) NOT EMCN" gene circuit in a co-culture assay with either SEM leukemia cells or EMCN$^+$ HSCs from primary human CD34-enriched bone marrow. We confirmed that CD34-enriched bone marrow samples used in this study included HSCs that expressed both EMCN (Figure S6A) and FLT3 (Figure S6B).

Both OR gate and OR-NOT gate CAR-NK cells killed cancer cells equally, reinforcing earlier results that, when not engaged, the iCAR does not tonically inhibit cytotoxicity (Figure 5E, left group, light green vs. medium green). Both OR gate and OR-NOT gate CAR-NK cells killed cancer cells slightly more than EMCN$^+$ HSCs, which is unsurprising due to NK cells' innately enhanced cytotoxicity against tumor cells (left vs. right group), which is one of the attributes NK cells possess that make them promising cell types for cell therapies. Crucially, however, the OR-NOT gate CAR-NK cells were significantly less toxic than OR gate CAR-NK cells toward primary EMCN$^+$ HSCs (Figure 5E, right group, light green vs. medium green; Figure S7), showing that the NOT gate can protect vulnerable primary healthy cells, potentially mitigating the risk of CAR-mediated, on-target/off-tumor toxicity. Within the context of well-established clinical protocols for hematopoietic cell transplantation, only a portion of the total normal HSC population is transplanted into conditioned transplant recipients, which is sufficient to provide long-term multi-lineage repopulation of an entire healthy hematopoietic system.[37,38] Consequently, it is likely that this level of NOT gate-mediated protection has the potential to be clinically impactful.

HSCs are the least differentiated hematopoietic cells and are capable of both self-renewal and multi-lineage repopulation. HSCs give rise to multi-potent progenitors (MPPs), which in turn give rise to all other lineages. Because MPPs express lower levels of EMCN than HSCs, we wanted to determine whether the EMCN iCAR still protected them, although any potential loss of MPPs would be reconstituted by HSCs, which are significantly protected by the iCAR (Figure 5E). We determined that OR-NOT-gated CAR-NK cells also significantly protected MPPs (Figure S9).

Finally, we aimed to confirm that the NOT gate can reduce on-target/off-tumor toxicity *in vivo*, using the full OR-NOT circuit with IL-15 support. To create an *in vivo* model for assessing on-target/off-tumor toxicity, we employed "on-tumor" and "off-tumor" cell lines that were FLT3$^+$CD33$^+$EMCN$^-$ and FLT3$^+$CD33$^+$EMCN$^+$, respectively. Both cell lines were based on endogenously FLT3$^+$ SEM cells modified to highly express CD33, but only "off-tumor" cells also exogenously expressed EMCN. Before engraftment, these two target cell subpopulations were mixed 1:1. In the following weeks, tumor burden was tracked via BLI of luciferase expressed by target cells. (Because both target cell subpopulations expressed the same luciferase cassette, BLI served only as a measurement of bulk killing.) To determine NOT gate function, peripheral blood was analyzed by flow cytometry to assess the relative abundance of each target subpopulation (Figure 6A). A functional OR-NOT circuit should result in an increase in the PA expression among target cells and a specific reduction in on-tumor cells.

The initial 50% PA expression among target cells was not appreciably changed by treating with untransduced NK cells (Figure 6B [representative examples], top row, right plot). When we injected control CAR-NK cells expressing the OR gate with a non-functional iCAR, we observed a drop in abundance of tumor cells relative to untransduced NK cells (Figure 6B, middle row, middle plot); however, the lack of a NOT gate in this circuit resulted in roughly equal proportions of on-tumor and off-tumor target cells (Figure 6B, middle row, right plot) due to indiscriminate cytotoxicity against both target populations. Notably, NK cells expressing the complete OR-NOT gate circuit resulted in precise ablation of the on-tumor target cell subpopulation, enriching the frequency of off-tumor target cells to over 90% of target cells (Figure 6B, third row, middle and right plots). To summarize, the OR-NOT gate resulted in a very significant enrichment of off-tumor target cells *in vivo*, while none of the other treatments resulted in any change from baseline (Figure 6C [group-averaged results], red box vs. others).

In terms of target cell abundance, OR-NOT gate CAR-NK cells significantly killed on-tumor cells beyond the level of innate killing of untransduced NK cells (Figure 6D, left). OR-NOT gate CAR-NK cells did not, however, exhibit CAR-mediated killing of off-tumor cells, while OR gate CAR-NK cells with a non-functional NOT gate exhibited substantial CAR-mediated on-target/off-tumor toxicity (Figure 6D, right). In other words, the addition of the NOT gate abolished CAR-mediated off-tumor cell killing *in vivo*. The NOT gate effect was also reflected in BLI (Figure S10A) and at other time points in the study (Figures S10B and S10C). The target cell PA expression and target cell abundance results, taken together, demonstrate that the OR-NOT gate can kill tumor cells while minimizing on-target/off-tumor toxicity *in vivo*.

DISCUSSION

Synthetic gene circuits afford the ability to engineer cells with complex, customizable phenotypes and input-output responses.[39–41] The field of logic-gated CARs is continuously

CellPress
OPEN ACCESS

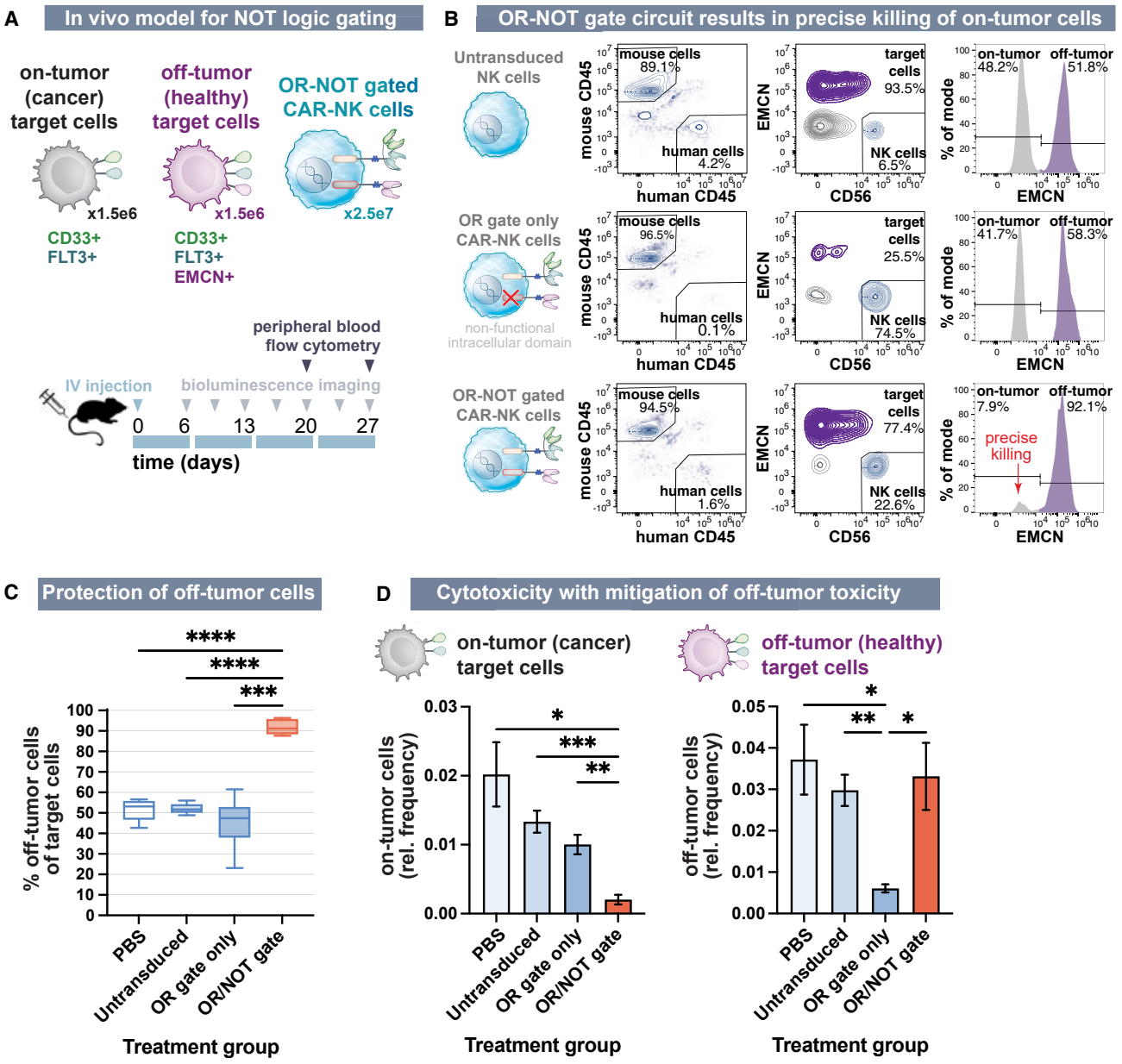

Figure 6. Triple-input OR-NOT gate CAR-NK cells avoid on-target/off-tumor toxicity *in vivo* with precise killing

(A) *In vivo* mixed target study design. "On-tumor" target cells (FLT3$^+$CD33$^+$EMCN$^-$ cancer model) and "off-tumor" target cells (FLT3$^+$CD33$^+$EMCN$^+$ healthy model) were mixed with NK cells and injected into mice.

(B) Peripheral blood was collected for flow-cytometry analysis of circulating target and NK cells. Representative data from each group illustrating identification of cell populations. Rows from top to bottom: untransduced NK cells; control NK cells expressing the OR gate CAR with a "dummy" iCAR containing a non-functional ICD; NK cells expressing full OR-NOT gate circuit. Columns from left to right: mouse vs. human cells; target vs. NK cells; on-tumor (gray) vs. off-tumor (purple) target cells. The OR-NOT gate potentiated precise killing of on-tumor cells (red arrow).

(C) Percentage of off-tumor target cells (of all target cells) in peripheral blood was specifically enriched by NK cells expressing the full OR-NOT gate circuit (red), day 20 post implantation. Box: interquartile range with line at median; whiskers: range of data.

(D) Target cell abundance (relative frequency among all CD45$^+$ cells) at day 27 post implantation. Left: OR-NOT gate CAR-NK cells (red) result in reduced frequency of on-tumor cells in peripheral blood via CAR-mediated killing. Right: without the NOT gate, OR gate CAR-NK cells (dark blue) kill off-tumor cells, but the full OR-NOT circuit (red) abolishes this toxicity.

Values represent the mean of at least five mice, and error bars represent ±SE of mean. In this figure, significance was tested using ANOVA (*$p < 0.05$, **$p < 0.01$, ***$p < 0.005$, ****$p < 0.001$).

expanding, and many individual "components" have already been described. Advances in the field today focus on combining these components into more complex, clinically oriented circuits. For example, inhibitory CARs have been designed in T cells and NK cells to create NOT gates, but they have not been combined with other logic-gated components to create larger circuits as we have here. Here, we demonstrate a synthetic three-input logic gate in NK cells, but it is also noteworthy as a therapeutic gene circuit in any cell type to target three clinically relevant antigens in a simultaneous, rather than sequential,[42] fashion. By protecting primary EMCN$^+$ HSCs, this therapeutic strategy has the potential to enable a wider therapeutic window for the treatment of AML and better post-treatment reconstitution of a healthy hematopoietic system, which would be medically meaningful if confirmed in clinical trials.

It has been proposed that the development of sophisticated cell therapies that sense, integrate, and respond to multiple ligand inputs will become increasingly common.[43,44] In developing such circuits, however, it can be problematic to measure their response only to individual target cell types presented separately. The experimental approach of artificially providing one type of target cell in isolation *in vitro* may be somewhat appropriate for modeling the physiological setting of some particularly homogeneous solid tumors, provided that cancerous and healthy tissues are sufficiently physically separate *in vivo*.[45] However, in heterogeneous tumors, which include liquid tumors (in which circulating cancer cells are invariably mixed with vulnerable healthy cells) and many solid tumors, the precision of killing will depend on fast-timescale decisions made by therapeutic cells. Switchable circuits based on protein-protein or protein-small molecule interactions[35,46–51] can signal faster than those based on gene expression[52–54] (for further discussion, see also Gordley et al.[55]). Our NOT gate distinguishes PA$^+$ from PA$^-$ target cells in a mixture potentially because ITIM signaling proceeds through protein recruitment and post-translational modification.[27] These data are also consistent with a model in which the iCAR works primarily in *cis*, rather than in *trans*, which is to say by responding to a PA on the same target cell that is already being targeted via an interaction between the aCAR and TAA. Since ITIM-based inhibitory receptors (including our iCARs) act by spatially recruiting phosphatases to the immune synapse, whereupon they locally dephosphorylate kinases associated with immune activation,[56] it follows that iCARs should primarily act at the same cell-cell interface as the aCAR's target.

The bivalent CAR demonstrated here can recognize two TAAs with one receptor and responds to target cells that are CD33$^+$, FLT3$^+$, or both. This is important in AML due to the heterogeneous nature of the disease, characterized by the presence of LSC and blast subpopulations with differing expression levels of these two antigens. Targeted therapies against CD33 have shown successful killing of AML blasts, but cases of relapse have occurred, likely due to residual LSCs that are low or negative for CD33. By targeting both FLT3 and CD33, we have shown that the OR gate described here can kill both primary blasts and LSCs, increasing its potential to control AML disease.

Interestingly, the extent of iCAR protection was revealed to be much higher in our *in vivo* experiments than initially suggested by overnight co-culture experiments. This might be due to the short timescale (1 day) and supraphysiological cell density in this standard *in vitro* assay format (i.e., high cell counts seeded in U-bottom plates that tend to accumulate cells at the bottom). In such conditions, activation of CAR-NK cells may be hyperstimulated, making it artificially difficult for the NOT gate to suppress cytotoxicity. The fact that NK cells exhibit a strong innate proclivity toward killing cancer cells may account for the superficially higher NOT gate protective effect in T cells in similarly artificial short-term *in vitro* assays using cancer cells to model "healthy cells."[57]

In the *in vitro* HSC protection experiments described herein, we chose a high density of cells in the assay to promote a high level of killing to facilitate measurement of the effect of the iCAR. This experimental design allowed us to successfully show that the iCAR significantly reduces toxicity toward HSCs, but, in a more physiological setting, this magnitude of killing would not occur. With this therapeutic strategy, critical HSC loss *in vivo* is unlikely because of NK cells' natural tendency to avoid killing normal cells (especially stem cells) under physiological conditions, HSCs' substantial capacity for self-renewal, and NK cell therapies' short-term persistence *in vivo*. Given the clinical success of current hematopoietic cell transplantation protocols,[37,38] the efficacy and protection aspects of our engineered OR-NOT CAR-NK cell circuit are promising for application toward AML.

We chose a short-term format for our HSC protection experiment because HSCs are not suitable for long-term experiments. This is because they tend to rapidly differentiate when cultured *ex vivo*, which drastically complicates the interpretability of the experiment. Long-term *in vivo* experiments using mouse models engrafted with human HSCs have similar pitfalls, including a paucity of bona fide, self-renewing HSCs after engraftment. For studying the system long term, here we instead leveraged an *in vivo* model using model cell lines, which confirmed that the NOT gate effect is even stronger over the longer term than observed in short-term *in vitro* experiments. *In vivo* studies with model cell lines are broadly used in the cell therapy and synthetic immunology fields, especially in logic gating studies where complex antigen combinations must be systematically tested *in vivo*.[42,45,47,52,58,59] The longer time frame and circulating environment of the *in vivo* experiments are likely to better reflect physiological settings and is where we observed the largest magnitude of effect. Another interesting observation was that the OR-NOT gate CAR-NK cells exhibit stronger cytotoxicity toward on-tumor cells compared to OR gate CAR-NK cells *in vivo*, possibly due to the latter cell type having to tackle both target cell types (PA$^+$ and PA$^-$), effectively reducing the effector-to-target (E/T) ratio. In our experiments, NOT-gated CAR-NK cells in the peripheral blood were low in frequency after several weeks, at which time the proportion of model healthy cells was >90% (Figure 6C) and comparable in abundance to our PBS treatment control (Figure 6D). These long-term data suggest that the kinetics of the system would preclude a collapse of the healthy cell population; instead, the margin of protected healthy cells widens over time.

Despite the artificial overexpression of EMCN in the model target cells, our data show that the level of protection is

comparable to primary HSCs with endogenous expression of EMCN, making it an informative model. The functional impact of comparatively "high" or "low" EMCN expression levels can only be understood in the context of the lineage and phenotype of the target cell. Our model cells are derived from tumor cells, which NK cells naturally tend to kill, whereas HSCs are primary stem cells that NK cells naturally tend to avoid. It follows that an artificially higher level of EMCN expression on tumor cells would be required to elicit a level of protection similar to that in endogenously EMCN^{+} HSCs.

An alternative mechanism for mitigating CAR toxicity is to kill the therapeutic cells through drug-[32] or antigen-inducible[60] expression of apoptotic effectors. Either strategy is undesirable with NK cells, due to challenges maintaining *in vivo* persistence.[61] The antigen-mediated kill switch is especially problematic if the death antigen is expressed in tissues that NK cells frequently visit after administration, such as the liver or lungs, in which case therapeutic cells may die altogether before reaching their true target. This strategy may further suffer if the timescale of CAR activation is faster than the kill switch, as is the case with transcription-based circuit components.[60] Because it is challenging to externally control cell behavior specifically in the vicinity of tumor cells, the drug-regulated version is more relevant to systemic toxicity, but, since NK cells, unlike T cells, rarely cause cytokine release syndrome or neurotoxicity, this approach may be of limited applicability. Compared to either approach, a key advantage of our iCAR-based NOT gate is the ITIM mechanism of action to directly inhibit the activating CAR through phosphatase intermediates rather than to compromise cell viability.

EMCN is broadly expressed on endothelial cells in addition to hematopoietic cells, meaning that the EMCN iCAR will likely be frequently engaged *in vivo* in different contexts. Unlike T cells, NK cells are part of innate immunity and use a "missing self" system for choosing targets. They express a large array of different inhibitory receptors that are continuously probing diverse ligands on various types of normal cells. Although they recognize a broad distribution of ubiquitous ligands (such as human leukocyte antigens, collagen, sialic acid, and lectins), many of these receptors share very similar ITIM-containing intracellular domains to LIR1 (e.g., KIRs, SIRPa, LAIR-1, SIGLECs, CEACAM-1, and other LIRs), meaning that NK cells normally receive ongoing signaling through these pathways (i.e., SHP-1, SHP-2, and SHIP-1). Indeed, it is central to NK cell maturation and function to be continually inhibited by healthy cells throughout all of the tissues that they traverse. Therefore, frequent stimulation of the LIR1 iCAR described here would not be expected to cause any abnormal outcomes in NK biology.

There are other logic gating strategies that can theoretically be employed to improve safety of CAR products. AND-gated CARs are theoretically only activated when two ligands are simultaneously detected on a target cell. One approach involves co-expression of two weak CARs recognizing different ligands: each engaged alone potentiates negligible activation, but ligating both creates additive or synergistic signaling that drives an above-threshold cytotoxic response.[46,47] Alternatively, a transcriptional switch responding to one antigen can be used to drive expression of a CAR recognizing a second, in which case killing only occurs when both antigens are present (although not simultaneously; see above regarding problems with slow kinetics being less amenable to discrimination).[59] In either case, the AND gate strategy is potentially more vulnerable to antigen escape, whereby cancer cells lose or downregulate expression of a TAA.[61] The two-antigen requirement of the AND gate gives cancer twice the opportunity to evade detection. NOT gates, on the other hand, rely on consistent PA expression on normal cells, which could potentially remain more stable than TAA expression on cancer cells, which is known to fluctuate, both over time and across tumor cells, especially under therapeutically exerted negative selection. Stability of PA expression on normal cells could hypothetically arise either from comparatively higher genetic stability of normal vs. cancer cells, from positive selection by effector cells, or from both.

Having demonstrated how this technology can be successfully applied within a liquid AML tumor setting, we are developing this circuit into a clinical candidate, SENTI-202, for patients with hematologic malignancies, including AML (clinical trial ID NCT06325748). Additionally, applying the OR-NOT gate circuit toward the treatment of solid tumors holds equally transformative potential. For example, anti-CEACAM5 engineered T cell approaches have demonstrated therapeutic potential in the clinic for the treatment of colorectal cancer; however, trials were halted due to off-tumor toxicity against the gastrointestinal tract[62] and possibly lung[63] tissues. We believe that such toxicity could be significantly reduced through the application of the NOT gate technology described in this work, potentially increasing the therapeutic window. Additionally, this circuit utilizes a form of IL-15, which could potentially be beneficial in the context of solid tumors by increasing the persistence and anti-tumor activity of NK (and other immune) cells within the immunosuppressive tumor microenvironment.

Limitations of the study

There remain avenues to further refine and understand NOT gate gene circuits in NK cells. Although we screened for high-performing, naturally occurring iCAR ICDs, we have not shown here any optimization of the "structural" domains of the iCAR, namely the hinge or transmembrane regions. Similarly, we focused solely on the 28z ICD for the mono- and OR-gated aCAR and did not elucidate here the effect of LIR1 iCARs on different aCAR co-stimulatory domains and their respective differential responses. Optimizing these parameters could be useful for refining both the function of these circuits and our understanding of them.

To further characterize the circuit *in vivo*, other animal models could also be employed. For example, NK cell injection could be delayed, allowing tumor cells to engraft further, which could make the sequence of events more closely resemble the clinical scenario of treating a patient. Although the extent of NOT gate function is likely to be similar, we anticipate that such a model may test the killing efficacy of the gene circuit more stringently, analogous to lowering the E/T ratio in an *in vitro* experiment.

STAR★METHODS

Detailed methods are provided in the online version of this paper and include the following:

SUPPLEMENTAL INFORMATION

Supplemental information can be found online at https://doi.org/10.1016/j.celrep.2024.114145.

ACKNOWLEDGMENTS

The authors would like to thank Wes Gorman and his team for their viral production support, Carmina Blanco for activating primary human NK cells, Tiffany Pan for additional characterization of EMCN expression, and the staff at Senti Biosciences for their support of the research and helpful review of the manuscript. This project has been funded in whole or in part with federal funds from the National Cancer Institute, National Institutes of Health, Department of Health and Human Services, under contract no. 75N91021C00026.

AUTHOR CONTRIBUTIONS

N.W.F.: conceptualization, formal analysis, supervision, visualization, writing – original draft, writing – review & editing, methodology, and project administration. H.D.: conceptualization, methodology, investigation, supervision, formal analysis, visualization, and project administration. G.Y.: investigation, supervision, formal analysis, and visualization. M.G.: investigation, formal analysis, and visualization. N.L.: investigation and visualization. A.L.: investigation and visualization. Y.L.: investigation and visualization. M.H.: conceptualization. D.L.: methodology. C.-T.L: investigation, supervision, and methodology. A.B.: investigation, formal analysis, and visualization. M.T.: investigation and methodology. N.A.: investigation. L.N.: investigation. A.R.: software. S.L.: conceptualization. W.W.: conceptualization. R.G.: supervision. T.K.L.: conceptualization and resources. B.G.: conceptualization, supervision, and project administration.

DECLARATION OF INTERESTS

N.W.F., H.D., G.Y., M.G., N.L., A.L., Y.L., M.H., D.L., C.-T.L., A.B., M.T., N.A., L.N., A.R., R.G., B.G., and T.K.L. are either current or former employees of Senti Biosciences, Inc., of which T.K.L. is also CEO and co-founder.

Received: August 21, 2023
Revised: March 25, 2024
Accepted: April 9, 2024

REFERENCES

1. Marofi, F., Al-Awad, A.S., Sulaiman Rahman, H., Markov, A., Abdelbasset, W.K., Ivanovna Enina, Y., Mahmoodi, M., Hassanzadeh, A., Yazdanifar, M., Stanley Chartrand, M., and Jarahian, M. (2021). CAR-NK Cell: A New Paradigm in Tumor Immunotherapy. Front. Oncol. *11*, 673276.
2. Sun, S., Hao, H., Yang, G., Zhang, Y., and Fu, Y. (2018). Immunotherapy with CAR-Modified T Cells: Toxicities and Overcoming Strategies. J. Immunol. Res. *2018*, 2386187. https://doi.org/10.1155/2018/2386187.
3. De Kouchkovsky, I., and Abdul-Hay, M. (2016). Acute myeloid leukemia: a comprehensive review and 2016 update. Blood Cancer J. *6*, e441. https://doi.org/10.1038/bcj.2016.50.
4. Gocek, E., and Marcinkowska, E. (2011). Differentiation therapy of acute myeloid leukemia. Cancers *3*, 2402–2420. https://doi.org/10.3390/cancers3022402.
5. Slats, A.M., Egeler, R.M., van der Does-van den Berg, A., Korbijn, C., Hählen, K., Kamps, W.A., Veerman, A.J.P., and Zwaan, C.M. (2005). Causes of death – other than progressive leukemia – in childhood acute lymphoblastic (ALL) and myeloid leukemia (AML): the Dutch Childhood Oncology Group experience. Leukemia *19*, 537–544. https://doi.org/10.1038/sj.leu.2403665.
6. (2022). Acute Myeloid Leukemia Treatment (PDQ®)–Health Professional Version - NCI. https://www.cancer.gov/types/leukemia/hp/adult-aml-treatment-pdq.
7. Yanada, M., Garcia-Manero, G., Borthakur, G., Ravandi, F., Kantarjian, H., and Estey, E. (2007). Potential cure of acute myeloid leukemia : analysis of 1069 consecutive patients in first complete remission. Cancer *110*, 2756–2760. https://doi.org/10.1002/cncr.23112.
8. Mangan, J.K., and Luger, S.M. (2011). Salvage Therapy for Relapsed or Refractory Acute Myeloid Leukemia. Ther. Adv. Hematol. *2*, 73–82. https://doi.org/10.1177/2040620711402533.
9. Sumide, K., Matsuoka, Y., Kawamura, H., Nakatsuka, R., Fujioka, T., Asano, H., Takihara, Y., and Sonoda, Y. (2018). A revised road map for the commitment of human cord blood CD34-negative hematopoietic stem cells. Nat. Commun. *9*, 2202. https://doi.org/10.1038/s41467-018-04441-z.
10. Molica, M., Perrone, S., Mazzone, C., Niscola, P., Cesini, L., Abruzzese, E., and de Fabritiis, P. (2021). CD33 Expression and Gentuzumab Ozogamicin in Acute Myeloid Leukemia: Two Sides of the Same Coin. Cancers *13*, 3214. https://doi.org/10.3390/cancers13133214.
11. Valent, P., Bauer, K., Sadovnik, I., Smiljkovic, D., Ivanov, D., Herrmann, H., Filik, Y., Eisenwort, G., Sperr, W.R., and Rabitsch, W. (2020). Cell-based and antibody-mediated immunotherapies directed against leukemic stem cells in acute myeloid leukemia: Perspectives and open issues. Stem Cells Transl. Med. *9*, 1331–1343. https://doi.org/10.1002/sctm.20-0147.
12. Bonardi, F., Fusetti, F., Deelen, P., van Gosliga, D., Vellenga, E., and Schuringa, J.J. (2013). A Proteomics and Transcriptomics Approach to Identify Leukemic Stem Cell (LSC) Markers. Mol. Cell. Proteomics *12*, 626–637. https://doi.org/10.1074/mcp.M112.021931.
13. Sachs, K., Sarver, A.L., Noble-Orcutt, K.E., LaRue, R.S., Antony, M.L., Chang, D., Lee, Y., Navis, C.M., Hillesheim, A.L., Nykaza, I.R., et al. (2020). Single-Cell Gene Expression Analyses Reveal Distinct Self-Renewing and Proliferating Subsets in the Leukemia Stem Cell Compartment in Acute Myeloid Leukemia. Cancer Res. *80*, 458–470. https://doi.org/10.1158/0008-5472.CAN-18-2932.
14. Ng, S.W.K., Mitchell, A., Kennedy, J.A., Chen, W.C., McLeod, J., Ibrahimova, N., Arruda, A., Popescu, A., Gupta, V., Schimmer, A.D., et al. (2016). A 17-gene stemness score for rapid determination of risk in acute leukaemia. Nature *540*, 433–437. https://doi.org/10.1038/nature20598.
15. Sitnicka, E., Buza-Vidas, N., Larsson, S., Nygren, J.M., Liuba, K., and Jacobsen, S.E.W. (2003). Human CD34+ hematopoietic stem cells capable of multilineage engrafting NOD/SCID mice express flt3: distinct flt3 and c-kit expression and response patterns on mouse and candidate human hematopoietic stem cells. Blood *102*, 881–886. https://doi.org/10.1182/blood-2002-06-1694.

16. Kikushige, Y., Yoshimoto, G., Miyamoto, T., Iino, T., Mori, Y., Iwasaki, H., Niiro, H., Takenaka, K., Nagafuji, K., Harada, M., et al. (2008). Human Flt3 Is Expressed at the Hematopoietic Stem Cell and the Granulocyte/Macrophage Progenitor Stages to Maintain Cell Survival. J. Immunol. *180*, 7358–7367. https://doi.org/10.4049/jimmunol.180.11.7358.

17. Sommer, C., Cheng, H.-Y., Nguyen, D., Dettling, D., Yeung, Y.A., Sutton, J., Hamze, M., Valton, J., Smith, J., Djuretic, I., et al. (2020). Allogeneic FLT3 CAR T Cells with an Off-Switch Exhibit Potent Activity against AML and Can Be Depleted to Expedite Bone Marrow Recovery. Mol. Ther. *28*, 2237–2251. https://doi.org/10.1016/j.ymthe.2020.06.022.

18. Karbowski, C., Goldstein, R., Frank, B., Kim, K., Li, C.-M., Homann, O., Hensley, K., Brooks, B., Wang, X., Yan, Q., et al. (2020). Nonclinical Safety Assessment of AMG 553, an Investigational Chimeric Antigen Receptor T-Cell Therapy for the Treatment of Acute Myeloid Leukemia. Toxicol. Sci. *177*, 94–107. https://doi.org/10.1093/toxsci/kfaa098.

19. Yeung, Y.A., Krishnamoorthy, V., Dettling, D., Sommer, C., Poulsen, K., Ni, I., Pham, A., Chen, W., Liao-Chan, S., Lindquist, K., et al. (2020). An Optimized Full-Length FLT3/CD3 Bispecific Antibody Demonstrates Potent Anti-leukemia Activity and Reversible Hematological Toxicity. Mol. Ther. *28*, 889–900. https://doi.org/10.1016/j.ymthe.2019.12.014.

20. Jetani, H., Garcia-Cadenas, I., Nerreter, T., Thomas, S., Rydzek, J., Meijide, J.B., Bonig, H., Herr, W., Sierra, J., Einsele, H., and Hudecek, M. (2018). CAR T-cells targeting FLT3 have potent activity against FLT3−ITD+ AML and act synergistically with the FLT3-inhibitor crenolanib. Leukemia *32*, 1168–1179. https://doi.org/10.1038/s41375-018-0009-0.

21. June, C.H., O'Connor, R.S., Kawalekar, O.U., Ghassemi, S., and Milone, M.C. (2018). CAR T cell immunotherapy for human cancer. Science *359*, 1361–1365. https://doi.org/10.1126/science.aar6711.

22. Pratap, S., and Zhao, Z.J. (2020). Finding new lanes: Chimeric antigen receptor (CAR) T-cells for myeloid leukemia. Cancer Rep. *3*, e1222. https://doi.org/10.1002/cnr2.1222.

23. Dannenfelser, R., Allen, G.M., VanderSluis, B., Koegel, A.K., Levinson, S., Stark, S.R., Yao, V., Tadych, A., Troyanskaya, O.G., and Lim, W.A. (2020). Discriminatory Power of Combinatorial Antigen Recognition in Cancer T Cell Therapies. Cell Syst. *11*, 215–228.e5. https://doi.org/10.1016/j.cels.2020.08.002.

24. Zah, E., Nam, E., Bhuvan, V., Tran, U., Ji, B.Y., Gosliner, S.B., Wang, X., Brown, C.E., and Chen, Y.Y. (2020). Systematically optimized BCMA/CS1 bispecific CAR-T cells robustly control heterogeneous multiple myeloma. Nat. Commun. *11*, 2283. https://doi.org/10.1038/s41467-020-16160-5.

25. Qin, H., Ramakrishna, S., Nguyen, S., Fountaine, T.J., Ponduri, A., Stetler-Stevenson, M., Yuan, C.M., Haso, W., Shern, J.F., Shah, N.N., and Fry, T.J. (2018). Preclinical Development of Bivalent Chimeric Antigen Receptors Targeting Both CD19 and CD22. Mol. Ther. Oncolytics *11*, 127–137. https://doi.org/10.1016/j.omto.2018.10.006.

26. Reckzeh, K., Kizilkaya, H., Helbo, A.S., Alrich, M.E., Deslauriers, A.G., Grover, A., Rapin, N., Asmar, F., Grønbæk, K., Porse, B., et al. (2018). Human adult HSCs can be discriminated from lineage-committed HPCs by the expression of endomucin. Blood Adv. *2*, 1628–1632. https://doi.org/10.1182/bloodadvances.2018015743.

27. Billadeau, D.D., and Leibson, P.J. (2002). ITAMs versus ITIMs: striking a balance during cell regulation. J. Clin. Invest. *109*, 161–168. https://doi.org/10.1172/JCI14843.

28. Fathi, E., Farahzadi, R., Sheervalilou, R., Sanaat, Z., and Vietor, I. (2020). A general view of CD33 $^{+}$ leukemic stem cells and CAR-T cells as interesting targets in acute myeloblatsic leukemia therapy. Blood Res. *55*, 10–16. https://doi.org/10.5045/br.2020.55.1.10.

29. Pollyea, D.A., and Jordan, C.T. (2017). Therapeutic targeting of acute myeloid leukemia stem cells. Blood *129*, 1627–1635. https://doi.org/10.1182/blood-2016-10-696039.

30. Liu, E., Tong, Y., Dotti, G., Shaim, H., Savoldo, B., Mukherjee, M., Orange, J., Wan, X., Lu, X., Reynolds, A., et al. (2018). Cord blood NK cells engineered to express IL-15 and a CD19-targeted CAR show long-term persistence and potent antitumor activity. Leukemia *32*, 520–531. https://doi.org/10.1038/leu.2017.226.

31. Marin, D., Li, Y., Basar, R., Rafei, H., Daher, M., Dou, J., Mohanty, V., Dede, M., Nieto, Y., Uprety, N., et al. (2024). Safety, efficacy and determinants of response of allogeneic CD19-specific CAR-NK cells in CD19+ B cell tumors: a phase 1/2 trial. Nat. Med. *30*, 772–784. https://doi.org/10.1038/s41591-023-02785-8.

32. Liu, E., Marin, D., Banerjee, P., Macapinlac, H.A., Thompson, P., Basar, R., Nassif Kerbauy, L., Overman, B., Thall, P., Kaplan, M., et al. (2020). Use of CAR-Transduced Natural Killer Cells in CD19-Positive Lymphoid Tumors. N. Engl. J. Med. *382*, 545–553. https://doi.org/10.1056/NEJMoa1910607.

33. Li, L., Mohanty, V., Dou, J., Huang, Y., Banerjee, P.P., Miao, Q., Lohr, J.G., Vijaykumar, T., Frede, J., Knoechel, B., et al. (2023). Loss of metabolic fitness drives tumor resistance after CAR-NK cell therapy and can be overcome by cytokine engineering. Sci. Adv. *9*, eadd6997. https://doi.org/10.1126/sciadv.add6997.

34. Daher, M., Basar, R., Gokdemir, E., Baran, N., Uprety, N., Nunez Cortes, A.K., Mendt, M., Kerbauy, L.N., Banerjee, P.P., Shanley, M., et al. (2021). Targeting a cytokine checkpoint enhances the fitness of armored cord blood CAR-NK cells. Blood *137*, 624–636. https://doi.org/10.1182/blood.2020007748.

35. Li, Y., Basar, R., Wang, G., Liu, E., Moyes, J.S., Li, L., Kerbauy, L.N., Uprety, N., Fathi, M., Rezvan, A., et al. (2022). KIR-based inhibitory CARs overcome CAR-NK cell trogocytosis-mediated fratricide and tumor escape. Nat. Med. *28*, 2133–2144. https://doi.org/10.1038/s41591-022-02003-x.

36. Imamura, M., Shook, D., Kamiya, T., Shimasaki, N., Chai, S.M.H., Coustan-Smith, E., Imai, C., and Campana, D. (2014). Autonomous growth and increased cytotoxicity of natural killer cells expressing membrane-bound interleukin-15. Blood *124*, 1081–1088. https://doi.org/10.1182/blood-2014-02-556837.

37. Konturek-Ciesla, A., and Bryder, D. (2022). Stem Cells, Hematopoiesis and Lineage Tracing: Transplantation-Centric Views and Beyond. Front. Cell Dev. Biol. *10*, 903528. https://doi.org/10.3389/fcell.2022.903528.

38. Khaddour, K., Hana, C.K., and Mewawalla, P. (2023). Hematopoietic Stem Cell Transplantation. In StatPearls (StatPearls Publishing).

39. Guye, P., Li, Y., Wroblewska, L., Duportet, X., and Weiss, R. (2013). Rapid, modular and reliable construction of complex mammalian gene circuits. Nucleic Acids Res. *41*, e156. https://doi.org/10.1093/nar/gkt605.

40. Hasty, J., McMillen, D., and Collins, J.J. (2002). Engineered gene circuits. Nature *420*, 224–230. https://doi.org/10.1038/nature01257.

41. Mansouri, M., and Fussenegger, M. (2022). Therapeutic cell engineering: designing programmable synthetic genetic circuits in mammalian cells. Protein Cell *13*, 476–489. https://doi.org/10.1007/s13238-021-00876-1.

42. Choe, J.H., Watchmaker, P.B., Simic, M.S., Gilbert, R.D., Li, A.W., Krasnow, N.A., Downey, K.M., Yu, W., Carrera, D.A., Celli, A., et al. (2021). SynNotch-CAR T cells overcome challenges of specificity, heterogeneity, and persistence in treating glioblastoma. Sci. Transl. Med. *13*, eabe7378. https://doi.org/10.1126/scitranslmed.abe7378.

43. Lim, W.A., and June, C.H. (2017). The Principles of Engineering Immune Cells to Treat Cancer. Cell *168*, 724–740. https://doi.org/10.1016/j.cell.2017.01.016.

44. Lee, S., Khalil, A.S., and Wong, W.W. (2022). Recent progress of gene circuit designs in immune cell therapies. Cell Syst. *13*, 864–873. https://doi.org/10.1016/j.cels.2022.09.006.

45. Srivastava, S., Salter, A.I., Liggitt, D., Yechan-Gunja, S., Sarvothama, M., Cooper, K., Smythe, K.S., Dudakov, J.A., Pierce, R.H., Rader, C., and Riddell, S.R. (2019). Logic-gated ROR1 chimeric antigen receptor expression rescues T cell-mediated toxicity to normal tissues and enables selective tumor targeting. Cancer Cell *35*, 489–503.e8. https://doi.org/10.1016/j.ccell.2019.02.003.

46. Cho, J.H., Okuma, A., Sofjan, K., Lee, S., Collins, J.J., and Wong, W.W. (2021). Engineering advanced logic and distributed computing in human

CAR immune cells. Nat. Commun. *12*, 792. https://doi.org/10.1038/s41467-021-21078-7.

47. Tousley, A.M., Rotiroti, M.C., Labanieh, L., Rysavy, L.W., Rietberg, S.P., de la Serna, E.L., Dalton, G.N., Klysz, D., Weber, E.W., Kim, W.-J., et al. (2022). Coopting T cell proximal signaling molecules enables Boolean logic-gated CAR T cell control. Preprint at bioRxiv. https://doi.org/10.1101/2022.06.17.496457.
48. Fedorov, V.D., Themeli, M., and Sadelain, M. (2013). PD-1- and CTLA-4-Based Inhibitory Chimeric Antigen Receptors (iCARs) Divert Off-Target Immunotherapy Responses. Sci. Transl. Med. *5*, 215ra172. https://doi.org/10.1126/scitranslmed.3006597.
49. Ng, A.H., Nguyen, T.H., Gómez-Schiavon, M., Dods, G., Langan, R.A., Boyken, S.E., Samson, J.A., Waldburger, L.M., Dueber, J.E., Baker, D., and El-Samad, H. (2019). Modular and tunable biological feedback control using a de novo protein switch. Nature *572*, 265–269. https://doi.org/10.1038/s41586-019-1425-7.
50. Giordano-Attianese, G., Gainza, P., Gray-Gaillard, E., Cribioli, E., Shui, S., Kim, S., Kwak, M.-J., Vollers, S., Corria Osorio, A.D.J., Reichenbach, P., et al. (2020). A computationally designed chimeric antigen receptor provides a small-molecule safety switch for T-cell therapy. Nat. Biotechnol. *38*, 426–432. https://doi.org/10.1038/s41587-019-0403-9.
51. Wu, C.-Y., Roybal, K.T., Puchner, E.M., Onuffer, J., and Lim, W.A. (2015). Remote control of therapeutic T cells through a small molecule-gated chimeric receptor. Science *350*, aab4077. https://doi.org/10.1126/science.aab4077.
52. Roybal, K.T., Williams, J.Z., Morsut, L., Rupp, L.J., Kolinko, I., Choe, J.H., Walker, W.J., McNally, K.A., and Lim, W.A. (2016). Engineering T Cells with Customized Therapeutic Response Programs Using Synthetic Notch Receptors. Cell *167*, 419–432.e16. https://doi.org/10.1016/j.cell.2016.09.011.
53. Scheller, L., Strittmatter, T., Fuchs, D., Bojar, D., and Fussenegger, M. (2018). Generalized extracellular molecule sensor platform for programming cellular behavior. Nat. Chem. Biol. *14*, 723–729. https://doi.org/10.1038/s41589-018-0046-z.
54. Daringer, N.M., Dudek, R.M., Schwarz, K.A., and Leonard, J.N. (2014). Modular Extracellular Sensor Architecture for Engineering Mammalian Cell-based Devices. ACS Synth. Biol. *3*, 892–902. https://doi.org/10.1021/sb400128g.
55. Gordley, R.M., Williams, R.E., Bashor, C.J., Toettcher, J.E., Yan, S., and Lim, W.A. (2016). Engineering dynamical control of cell fate switching using synthetic phospho-regulons. Proc. Natl. Acad. Sci. USA *113*, 13528–13533. https://doi.org/10.1073/pnas.1610973113.
56. Stebbins, C.C., Watzl, C., Billadeau, D.D., Leibson, P.J., Burshtyn, D.N., and Long, E.O. (2003). Vav1 Dephosphorylation by the Tyrosine Phosphatase SHP-1 as a Mechanism for Inhibition of Cellular Cytotoxicity. Mol. Cell Biol. *23*, 6291–6299. https://doi.org/10.1128/MCB.23.17.6291-6299.2003.
57. Hamburger, A.E., DiAndreth, B., Cui, J., Daris, M.E., Munguia, M.L., Deshmukh, K., Mock, J.-Y., Asuelime, G.E., Lim, E.D., Kreke, M.R., et al. (2020). Engineered T cells directed at tumors with defined allelic loss. Mol. Immunol. *128*, 298–310. https://doi.org/10.1016/j.molimm.2020.09.012.
58. Tokatlian, T., Asuelime, G.E., Mock, J.-Y., DiAndreth, B., Sharma, S., Toledo Warshaviak, D., Daris, M.E., Bolanos, K., Luna, B.L., Naradikian, M.S., et al. (2022). Mesothelin-specific CAR-T cell therapy that incorporates an HLA-gated safety mechanism selectively kills tumor cells. J. Immunother. Cancer *10*, e003826. https://doi.org/10.1136/jitc-2021-003826.
59. Roybal, K.T., Rupp, L.J., Morsut, L., Walker, W.J., McNally, K.A., Park, J.S., and Lim, W.A. (2016). Precision Tumor Recognition by T Cells With Combinatorial Antigen-Sensing Circuits. Cell *164*, 770–779. https://doi.org/10.1016/j.cell.2016.01.011.
60. Williams, J.Z., Allen, G.M., Shah, D., Sterin, I.S., Kim, K.H., Garcia, V.P., Shavey, G.E., Yu, W., Puig-Saus, C., Tsoi, J., et al. (2020). Precise T cell recognition programs designed by transcriptionally linking multiple receptors. Science *370*, 1099–1104. https://doi.org/10.1126/science.abc6270.
61. Majzner, R.G., and Mackall, C.L. (2018). Tumor Antigen Escape from CAR T-cell Therapy. Cancer Discov. *8*, 1219–1226. https://doi.org/10.1158/2159-8290.CD-18-0442.
62. Parkhurst, M.R., Yang, J.C., Langan, R.C., Dudley, M.E., Nathan, D.-A.N., Feldman, S.A., Davis, J.L., Morgan, R.A., Merino, M.J., Sherry, R.M., et al. (2011). T Cells Targeting Carcinoembryonic Antigen Can Mediate Regression of Metastatic Colorectal Cancer but Induce Severe Transient Colitis. Mol. Ther. *19*, 620–626. https://doi.org/10.1038/mt.2010.272.
63. Thistlethwaite, F.C., Gilham, D.E., Guest, R.D., Rothwell, D.G., Pillai, M., Burt, D.J., Byatte, A.J., Kirillova, N., Valle, J.W., Sharma, S.K., et al. (2017). The clinical efficacy of first-generation carcinoembryonic antigen (CEACAM5)-specific CAR T cells is limited by poor persistence and transient pre-conditioning-dependent respiratory toxicity. Cancer Immunol. Immunother. *66*, 1425–1436. https://doi.org/10.1007/s00262-017-2034-7.
64. Knorr, K.L.B., Finn, L.E., Smith, B.D., Hess, A.D., Foran, J.M., Karp, J.E., and Kaufmann, S.H. (2017). Assessment of Drug Sensitivity in Hematopoietic Stem and Progenitor Cells from Acute Myelogenous Leukemia and Myelodysplastic Syndrome Ex Vivo. Stem Cells Transl. Med. *6*, 840–850. https://doi.org/10.5966/sctm.2016-0034.

STAR★METHODS

KEY RESOURCES TABLE

REAGENT or RESOURCE	SOURCE	IDENTIFIER
Antibodies		
Mouse monoclonal anti-V5 tag Alexa Fluor 647	Life Technologies	451098
Rat monoclonal anti-FLAG Brilliant Violet 421	BioLegend	637321
Mouse monoclonal anti-Myc-tag Alexa Fluor 488	Cell Signaling Technology	2279S
Mouse monoclonal Anti-Human IL-15 Biotin	BD Biosciences	554713
Mouse monoclonal anti-human CD56 Brilliant Violet 650	BioLegend	362532
Mouse monoclonal anti-human CD34 FITC	BioLegend	343504
Mouse anti-human lineage cocktail APC	BioLegend	348803
Mouse monoclonal anti-human CD38 BUV395	BD Biosciences	563811
Mouse monoclonal anti-human CD45RA BUV737	BD Biosciences	612846
Mouse monoclonal anti-human CD33 PE	BD Biosciences	555450
Mouse monoclonal Mouse monoclonal anti-human CD90 Brilliant Violet 421	BioLegend	405225
Mouse monoclonal Anti-mouse CD45-PerCP-Cy5.5	BioLegend	103132
Mouse monoclonal Anti-human CD45 PE	BioLegend	304008
Mouse monoclonal Anti-human CD56 APC	BioLegend	318310
Bacterial and virus strains		
Ready-to-Use Lentiviral Packaging Plasmid Mix	Cellecta, Inc.	CPCP-K2A
Biological samples		
AML BMMC, Cryo, Blast >20%	Discovery Life Sciences	100030.2
$CD34^+$ BMMCs	AllCells	$CD34^+$ PS
Chemicals, peptides, and recombinant proteins		
Zombie UV	BioLegend	423108
SYTOX Red	Invitrogen	S34859
PE Streptavidin	BioLegend	504204
CellTrace Violet	Invitrogen	C34557
FuGENE	Promega	E2311
PEI MAX® MW 40,000	PolySciences	24765
D-Luciferin	Gold Biotechnology	LUCK-5G
RBC Lysis Buffer (10X)	BioLegend	420301
DNAse I	Millipore Sigma	11284932001
2-mercaptoethanol	Gibco	21985023
Stem Cell Factor	R&D systems	255-SC
IL-3	R&D systems	203-IL
GM-CSF	R&D systems	7954-GM
G-CSF	R&D systems	214-CS
Erythropoietin	Millipore Sigma	11120166001
Transferrin	Millipore Sigma	10652202001
Critical commercial assays		
Human ProcartaPlex Mix&Match 6-Plex Immunoassay	Invitrogen	PPX-06-MXMFYNN

(*Continued on next page*)

Continued

REAGENT or RESOURCE	SOURCE	IDENTIFIER
Deposited data		
Affymetrix Human Genome U133 Plus 2.0 Array datasets (various)	Gene Expression Omnibus (https://www.ncbi.nlm.nih.gov/geo/)	GSE13159, GSE15434, GSE17054, GSE24006, GSE28490, GSE28491, GSE42519, GSE49910, GSE63270, GSE6891, GSE93777
Human (NCBITaxon:9606) "cell surface" proteins	Gene Ontology Resource (https://geneontology.org)	GO:0009986
Human (NCBITaxon:9606) "membrane" proteins	Gene Ontology Resource (https://geneontology.org)	GO:0016020
Antibody-based annotations of protein localization	Human Protein Atlas (https://www.proteinatlas.org/)	N/A
AML bulk RNAseq data	https://www.cancer.gov/ccg/research/genome-sequencing/tcga	N/A
The gene and gene product information of KLRG1	Uniprot (https://www.uniprot.org/)	Q96E93
The gene and gene product information of BTLA	Uniprot (https://www.uniprot.org/)	Q7Z6A9
The gene and gene product information of KIR3DL1	Uniprot (https://www.uniprot.org/)	P43629
The gene and gene product information of NKG2A	Uniprot (https://www.uniprot.org/)	P26715
The gene and gene product information of SIGLEC-2	Uniprot (https://www.uniprot.org/)	P20273
The gene and gene product information of SIGLEC-10	Uniprot (https://www.uniprot.org/)	Q96LC7
The gene and gene product information of LIR-2	Uniprot (https://www.uniprot.org/)	Q8N423
The gene and gene product information of LIR-3	Uniprot (https://www.uniprot.org/)	O75022
The gene and gene product information of LAIR1	Uniprot (https://www.uniprot.org/)	Q6GTX8
The gene and gene product information of KIR2DL1	Uniprot (https://www.uniprot.org/)	P43626
The gene and gene product information of LIR1	Uniprot (https://www.uniprot.org/)	Q8NHL6
The gene and gene product information of CD33	Uniprot (https://www.uniprot.org/)	P20138
The gene and gene product information of FLT3	Uniprot (https://www.uniprot.org/)	P36888
The gene and gene product information of EMCN	Uniprot (https://www.uniprot.org/)	Q9ULC0
Experimental models: Cell lines		
Human: SEM (ALL, female)	DSMZ	ACC 546
Human: MOLM13 (AML, male)	AddexBio	C0003003
Human: MV4-11 (AML/ALL, male)	ATCC	CRL-9591
Human: Lenti-X 293T (transformed, female)	Takara	632180
Human: GP2-293 (transformed, female)	Takara	631458
Experimental models: Organisms/strains		
NOD.Cg-*Prkdc*^{scid} *Il2rg*^{tm1Wjl} Tg(IL15)1Sz/SzJ	Jackson Laboratories	030890
Recombinant DNA		
Gene circuit constructs	This paper	N/A
Antigen expression constructs	This paper	N/A
Software and algorithms		
Prism	GraphPad	https://www.graphpad.com/scientific-software/prism/

RESOURCE AVAILABILITY

Lead contact

Requests for further information should be directed to the lead contact, Brian Garrison (brian.garrison@sentibio.com).

Materials availability

Requests for information regarding plasmids and cell lines generated in this study should be directed to the lead contact, Brian Garrison (brian.garrison@sentibio.com). Some materials may not be available as they are proprietary to Senti Biosciences.

Data and code availability

- Requests for data generated in this study should be directed to the lead contact. Senti may disclose certain analyzed data at its sole discretion and subject to Senti and the requester being able to enter into a written agreement as required by Senti.
- This paper does not report original code.
- Any additional information required to reanalyze the data reported in this paper is available from the lead contact, subject to the abovementioned conditions.

EXPERIMENTAL MODEL AND STUDY PARTICIPANT DETAILS

NK cell engineering

Primary NK cells were isolated from PBMCs from healthy donors and frozen in liquid nitrogen. Male and female donors were used interchangeably with no noticeable difference. For individual experiments, single vials of frozen NK cells were thawed and stimulated with irradiated feeder cells (K562 cells engineered to express membrane bound IL-21 and membrane bound IL-15). NK cells were expanded in 6-well plates in NK media (NK MACS media with 5% human AB serum with 10 ng/mL IL-15 and 100 U/mL IL-2) at a cell concentration range of 5e5 to 1e6 cells/mL. After 10 days of expansion, cultures were analyzed by flow cytometry to ensure a lack of residual feeder cells or $CD3^+$ cells.

Cell lines

SEM and MOLM13 were cultured in RPMI (VWR Life Sciences) with 10% FBS (Seradigm) and 1% Penicillin-Streptomycin (Gibco) and MV4-11 cells were cultured in IMDM (Gibco) with 10% FBS and 1% Penicillin-Streptomycin. All cells were cultured at 37°C and 5% CO_2. To create $CD33^+fluc^+$ SEM target cells, 100 μL of lentiviral supernatant of a construct encoding constitutive expression of CD33, fLuc, and blasticidin resistance was applied to 0.5e6 SEM cells and incubated for 2–3 days. Transductants were enriched using 4 μg/mL blasticidin for 1 week. To create EMCN-expressing variants, either parental SEM cells or $CD33^+$ SEM cells were similarly transduced with a lentiviral vector constitutively co-expressing EMCN, GFP, and a puromycin resistance cassette as above, and 2 μg/mL puromycin was used for enrichment. Lenti-X 293T or GP2-293 were cultured in DMEM (Gibco) with 1 mM Sodium Pyruvate (Gibco), 10% FBS, 1% Penicillin-Streptomycin.

Primary cells

Frozen bone marrow samples from AML patients (Discovery Life Sciences, Inc.) were thawed, treated with DNAse I (Millipore Sigma), washed, and cultured overnight in RPMI media supplemented with 10% fetal bovine serum, 0.055 mM 2-mercaptoethanol (Gibco), 3 ng/mL stem cell factor (R&D systems), 20 ng/mL IL-3 (R&D systems), 200 μg/ml Transferrin (Millipore Sigma), 20 ng/mL GM-CSF (R&D systems), 10 ng/mL G-CSF (R&D systems), 3 U/ml erythropoietin (Millipore Sigma) prior to being washed in assay medium, counted, and added to cytotoxicity assays. Male and female donors were used interchangeably with no apparent difference. CD34-enriched bone marrow cells from healthy donors (AllCells, LLC) were thawed and immediately washed in assay media, counted, and added to a cytotoxicity assay. Male and female donors were used interchangeably with no apparent difference.

In vivo models

Five-week-old female NOD.Cg-*Prkdc*^{scid} *Il2rg*^{tm1Wjl} Tg(IL15)1Sz/SzJ mice were purchased from The Jackson Laboratory. On arrival, these mice were socially housed in single-use polycarbonate cages. These cages were housed in individually ventilated Innovive IVC rodent racks. Sterilized ALPHA-dri bedding, sterilized water, and irradiated Teklad global soy protein-free extruded rodent diet were provided in each cage. All animal procedures were performed in strict accordance with the recommendations in the Guide for the Assessment and Accreditation of Laboratory Animal Care International. The protocol was approved by the Institutional Animal Care and Use Committee (IACUC) of Explora Biolabs. Mice were engrafted with cancer cell lines via tail vein injection on day 0. For OR gate studies, either MOLM13 cells (1e5) or SEM cells (5e6) was used. For OR-NOT gate studies, a mixture of 1.5e6 SEM $CD33^+$ and 1.5e6 SEM $CD33^+EMCN^+$ cells was used. At least 6 mice were used per group.

METHOD DETAILS

Bioinformatic pipelines

Affymetrix Human Genome U133 Plus 2.0 Array datasets corresponding to cell types of interest were obtained from GEO (https://www.ncbi.nlm.nih.gov/geo/). The following datasets were used: GSE13159, GSE15434, GSE17054, GSE24006, GSE28490, GSE28491, GSE42519, GSE49910, GSE63270, GSE6891, GSE93777. Data was Robust Multichip Average normalized and expression values were extracted. A set of 7,680 membrane and cell surface proteins was derived using GO (using Gene Ontology terms "cell surface" and "membrane") and HPA (Human protein Atlas, antibody-based annotations) from a set of 20,216 protein coding

genes (NCBI). Of those, 115 displaying higher expression in hematopoietic stem cells (HSCs) compared to AML were selected using microarray data (1,128 samples and 13,744 probes representing 882 AML associated samples and 246 samples of normal blood cell types after removing outlier and low-correlating data). Statistically significant hits (t test) were ranked by fold change to isolate potential NOT gate targets. Of these genes, 15 were confirmed to be expressed at low levels in AML using bulk RNAseq data (TCGA) and one of them (EMCN) was selected after manual curation incorporating literature sources.

NK cell engineering

Constructs were first designed in silico (SnapGene), after which DNA was synthesized (Genscript) and reprepped as needed (Genewiz). We used pL17d as the lentiviral backbone for smaller constructs and SINvec and retrovec as the gamma retroviral backbones for larger constructs. Constructs used in this publication were designed by combining sequence fragments exactly as shown in the main text figures, except as noted below. Among these fragments, naturally occurring sequences were acquired either from publicly available sequences (Uniprot) or cDNA clones (Genscript), and scFv binder sequences were either sourced from NCI (FLT3, CD33, HER2) or internally generated (EMCN). For iCAR validation and screening (Figure 3), aCARs and iCARs were expressed from separate lentiviral constructs. The iCAR constructs also included a puromycin resistance gene (not diagrammed), which was placed after the receptor gene separated by a 2A ribosomal skip sequence. FLAG (single target) and myc (OR gate) were used as epitope tags on aCARs, and V5 was used as an epitope tag on iCARs. To create multicistronic constructs (OR-NOT gate), receptor chains were linked together with 2A ribosomal skip sequences in one retroviral vector. DNA was transfected into Lenti-X 293T (lentivirus) or GP2-293 (gamma retrovirus) cells using either FuGENE or PEI, respectively, following manufacturer recommendations. Viral supernatant was collected from these cultures, clarified by centrifugation, and concentrated using either Lenti-X concentrator (smaller batches for *in vitro* experiments) or Amicon spin filters followed by $MgCl_2$ and benzonase treatment (larger batches for *in vivo* experiments), according to manufacturer recommendations and standard practices. Twelve-well plates were coated with recombinant human fibronectin fragment (RetroNectin, Cat#T100B) according to manufacturer protocols. NK cells and lentivirus or retrovirus were added to coated plates and centrifuge at 1000g for 2 h at 32°C. After 3 days, media was exchanged for NK media (for iCAR screening, 2 μg/mL puromycin was added). After 4 more days, receptor expression was checked by flow cytometry (for staining reagents, see Table S1) and cells were harvested for use in assays. For *in vivo* experiments, cells were transferred to 6-well G-Rex (Wilson Wolf, CAT#MSPP-80660M) for further expansion post-transduction.

In vitro cytotoxicity assay setup

At day 7 post-transduction, NK cells were washed twice in assay medium (RPMI [VWR Life Sciences] with 10% FBS [Seradigm]) and plated in 96-well U-bottom plates. Co-cultures of 5e4 target cells and 2.5e4 NK cells in a total volume of 200 μL of assay medium were incubated for 16–20 h, after which plates were analyzed on a Beckman CytoFLEX flow cytometer. For cell line experiments, target cells were stained with CellTrace Blue (Invitrogen) according to manufacturer protocols and resuspended in assay medium prior to starting the co-culture. After the co-culture, plates were centrifuged and 100 μL supernatant was set aside for cytokines to be quantified using Luminex assays according to manufacturer protocols. Co-cultures were then stained with Sytox Red (Invitrogen) and the number of live target cell events in a fixed volume was recorded. For AML patient bone marrow experiments, CellTrace and Sytox were not used; rather, co-cultures were instead stained with an antibody cocktail: non-NK cells were separated by low CD56 expression, AML blast cells were identified by low CD45 expression and low side scatter, and LSCs were identified by a $CD34^+CD38^-$ phenotype (Table S2). Experiments with $CD34^+$ bone marrow were performed similarly, except that IL-15 was added to OR gate control to compensate for the IL-15 expressed by the OR-NOT gate circuit, and a different antibody staining panel was used for immunophenotyping[64] (Table S2; Figure S7).

In vivo studies

At day 12 post-transduction, NK cells were collected from the 6M G-rex, washed, and counted for *in vivo* injection. NK cells (3.5e7 for OR gate; 2.5e7 for OR-NOT gate) were injected via tail vein at day 0. For OR gate studies, either Molm13 cells (1e5) or SEM cells (5e6) was used. For OR-NOT gate studies, a mixture of 1.5e6 SEM $CD33^+$ and 1.5e6 SEM $CD33^+EMCN^+$ cells was used. Bioluminescence imaging was performed using a Lago Imager (Spectral Instruments) twice weekly. Mice were injected with 200 μL of D-luciferin (150 mg/kg, Gold Biotechnology Inc, LUCK-5G) and imaged 10 min later. For OR-NOT gate experiments, peripheral blood was collected once a week by submental bleeding into EDTA tubes (Vacuette Minicollect 0.5 mL, Greiner, CAT#450474), of which 150–200 μL of blood was processed per mouse for flow cytometry analysis using 7 mL red blood cell lysis buffer (Biolegend CAT#420302) for 5 min, followed by quenching with 7 mL FACS buffer (FBS: Avantor 89510-186; EDTA: EMD Millipore 324506; DPBS: Cytiva SH30028.02). This process was repeated and followed with a final FACS buffer wash, followed by antibody staining (Table S3).

QUANTIFICATION AND STATISTICAL ANALYSIS

Visualization and statistics

Data visualization and statistical analysis was performed using Prism (ver. 9). We used Brown-Forsythe ANOVA for comparisons of multiple groups and Welch's test for two-group comparisons, with p-values annotated as $^*p < 0.5$, $^{**}p < 0.01$, $^{***}p < 0.005$, $^{****}p < 0.001$. For visualizing summary statistics, we used the arithmetic mean and standard error of the mean.

In vitro cytotoxicity quantification from flow cytometry-based cell counting

Killing described as "aCAR mediated" was calculated by subtracting basal killing from total killing. Total killing was defined as the percent reduction of target cell counts with NK cells relative to without. Basal killing was defined as the total killing specifically with "control NK cells" lacking an aCAR. When puromycin selection was used to enrich NOT gate CAR-NK cells, "control NK cells" were transduced with iCAR alone and selected in the same manner. In all other cases, untransduced NK cells served as "control NK cells." All measurements were performed in technical triplicate. Results were robust to multiple biological replicates (Figure S2C) and different NK cell donors (Figure S8A).

Cell Reports, Volume *43*

Supplemental information

Precision off-the-shelf natural killer cell therapies for oncology with logic-gated gene circuits

Nicholas W. Frankel, Han Deng, Gozde Yucel, Marcus Gainer, Nelia Leemans, Alice Lam, Yongshuai Li, Michelle Hung, Derrick Lee, Chen-Ting Lee, Andrew Banicki, Mengxi Tian, Niran Almudhfar, Lawrence Naitmazi, Assen Roguev, Seunghee Lee, Wilson Wong, Russell Gordley, Timothy K. Lu, and Brian S. Garrison

Supplemental information

target	antibody	manufacturer	catalog number
iCAR	anti-V5 tag mouse mAB	Life Technologies	451098
aCAR (iCAR screen)	anti-FLAG rat mAb	Biolegend	637321
aCAR (OR and OR-NOT gate)	anti-Myc-tag mouse mAb	Cell Signaling Technology	2279S
Dead cells	SYTOX Red	Invitrogen	S34859
Tumor cells	CellTrace Violet	Invitrogen	C34557
IL-15	Biotin Mouse Anti-Human IL-15	BD Biosciences	554713
	PE Streptavidin	Biolegend	504204

Table S1. Staining panel for gene circuit expression and cell line assays

target	antibody	manufacturer	catalog number
CD56	anti-human CD56 antibody	Biolegend	362532
CD34	anti-human CD34 antibody	Biolegend	343504
Differentiated cells	anti-human lineage cocktail	Biolegend	348803
Dead cells	SYTOX Red	Invitrogen	S34859
CD38	anti-human CD38 antibody	BD Biosciences	563811
CD45RA	anti-human CD45RA antibody	Biolegend	612846
CD33	anti-human CD33 antibody	BD Biosciences	555450
CD90	anti-human CD90 antibody	Biolegend	405225

Table S2. Staining panel for HSPC subpopulations

target	antibody	manufacturer	catalog number
Dead cells	Zombie UV	Biolegend	423108
Mouse cells	Anti-mouse CD45-PerCP-Cy5.5	Biolegend	103132
Human cells	Anti-human CD45 PE	Biolegend	304008
NK cells	Anti-human CD56 APC	Biolegend	318310
EMCN	GFP (co-expressed with EMCN)	n/a	n/a

Table S3. Staining panel for peripheral blood samples from OR-NOT gate CAR-NK cell mouse studies

abbreviation	Cell type name
AML LSCs	AML leukemic stem cells CD34+CD38-.[11,12,29]
HSCs	hematopoietic stem cells Lin-CD34+CD38-CD45RA-CD90-.[65,66]
LPMPs	lymphoid-primed multipotent progenitors
CMPs	common myeloid progenitor
GMPs	granulocyte/macrophage progenitors
MEPs	megakaryocyte/erythrocyte progenitors
PMs	promyelocyte
MYs	myelocyte
MMs	metamyelocyte
PMNs	polymorphonuclear cells
DCs	dendritic cells
BM	bone marrow

Table S4. Abbreviations used in this study and key immunophenotypes.

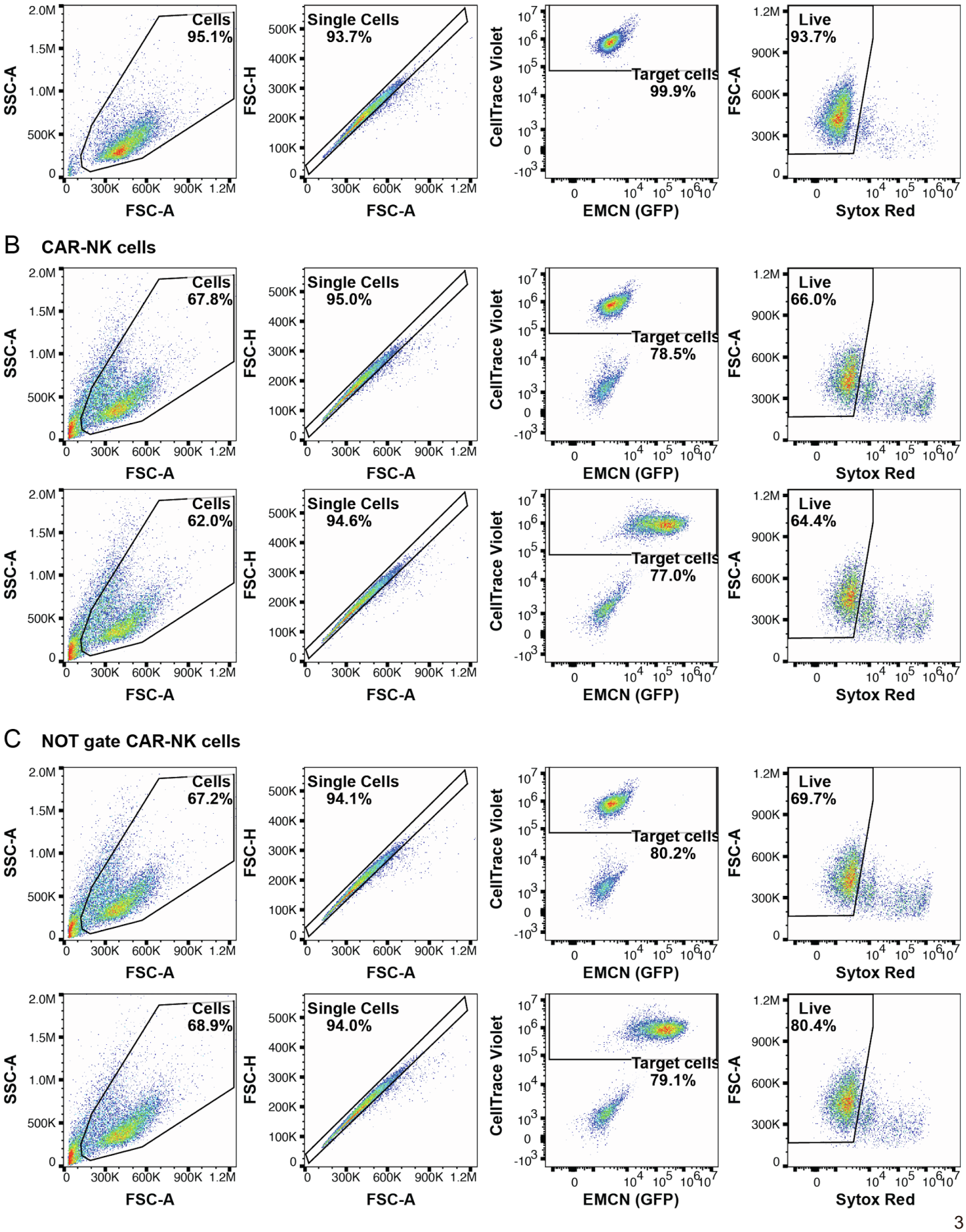
A
No NK cells
Cells
95.1%
Single Cells
93.7%
Target cells
99.9%
Live
93.7%
B
CAR-NK cells
Cells
67.8%
Single Cells
95.0%
Target cells
78.5%
Live
66.0%
Cells
62.0%
Single Cells
94.6%
Target cells
77.0%
Live
64.4%
C
NOT gate CAR-NK cells
Cells
67.2%
Single Cells
94.1%
Target cells
80.2%
Live
69.7%
Cells
68.9%
Single Cells
94.0%
Target cells
79.1%
Live
80.4%
SSC-A
FSC-A
FSC-H
CellTrace Violet
EMCN (GFP)
Sytox Red

Figure S1 (previous page). Gating strategy for quantifying in vitro killing assay. A representative example of each condition is shown From left to right, progressive gating based on cell size/granularity, single cells, CellTrace-stained endogenously FLT3+ SEM target cells, and Sytox-negative live cells CellTrace-negative cells are NK cells. The last gate was used to count the number of live target cells for the purpose of killing quantification (Methods). A. A baseline target cell number was established by adding no NK cells. B. Addition of anti-FLT3 CAR-NK cells reduced count and viability of both $EMCN^{-}$ (top row) and $EMCN^{+}$ (bottom row) target cells to an equal extent, demonstrating no aFLT3 CAR-NK cell response to the protective antigen EMCN (engineered expression, co-expressed with GFP). CellTrace-negative cells are NK cells. C. FLT3 NOT EMCN circuit in NOT gate CAR-NK cells protects $EMCN^{+}$ target cells (bottom row, as compared to top row), reflecting iCAR-mediated inhibition of aCAR-mediated killing in a protective antigen-dependent manner. FSC: Forward scatter; SSC: Side scatter; -A: area of signal; -H: height of signal.

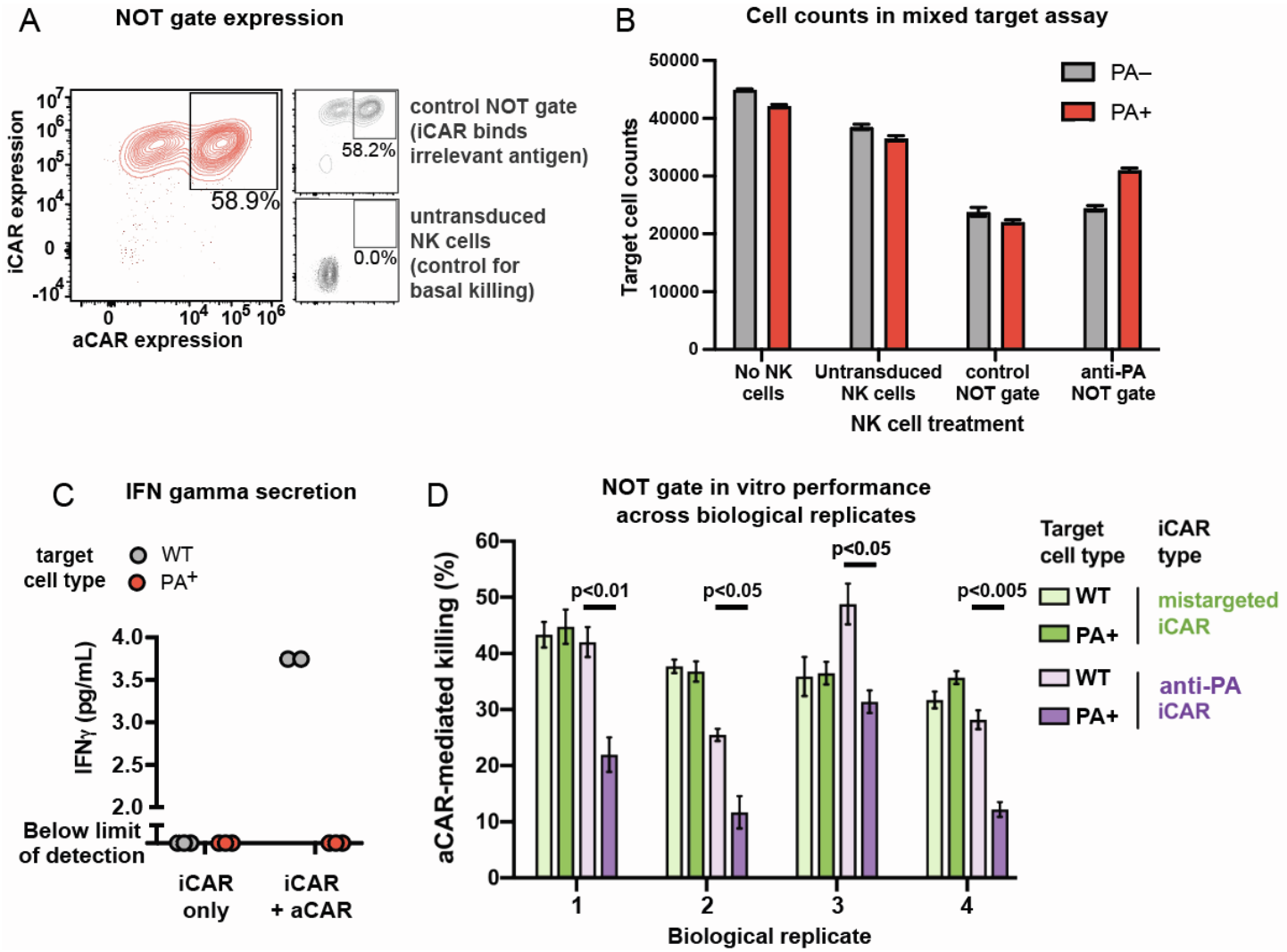

Figure S2. NOT gate expression and robustness. A. Representative example of aCAR and iCAR co-expression NK cells. Gate for double positive expression set based on untransduced NK cells. Double positive frequency is comparable between FLT3 NOT EMCN circuit (left) and the control FLT3 NOT HER2 circuit, in which the iCAR recognizes an off-target antigen, HER2, not expressed on any target cells in the assay, instead of EMCN (top right). B. Raw target cell counts corresponding to the mixed target cell experiment in Figure 3D. C. Interferon gamma secreted by NK cells expressing aEMCN iCAR with or without aFLT3 aCAR in response to parental, endogenously FLT3$^+$ SEM cells (WT) or SEM cells over-expressing of EMCN (PA$^+$). Values of 2 or 3 replicates are shown. D. Multiple biological replicates of results in Figure 1F showed consistently statistically significant iCAR-mediated suppression of aCAR-mediated killing in a PA-dependent manner. Values represent the mean of 3 technical replicates and error bars represent ± S.E.M. Statistical test: Welch's t-test between green bars and between purple bars.

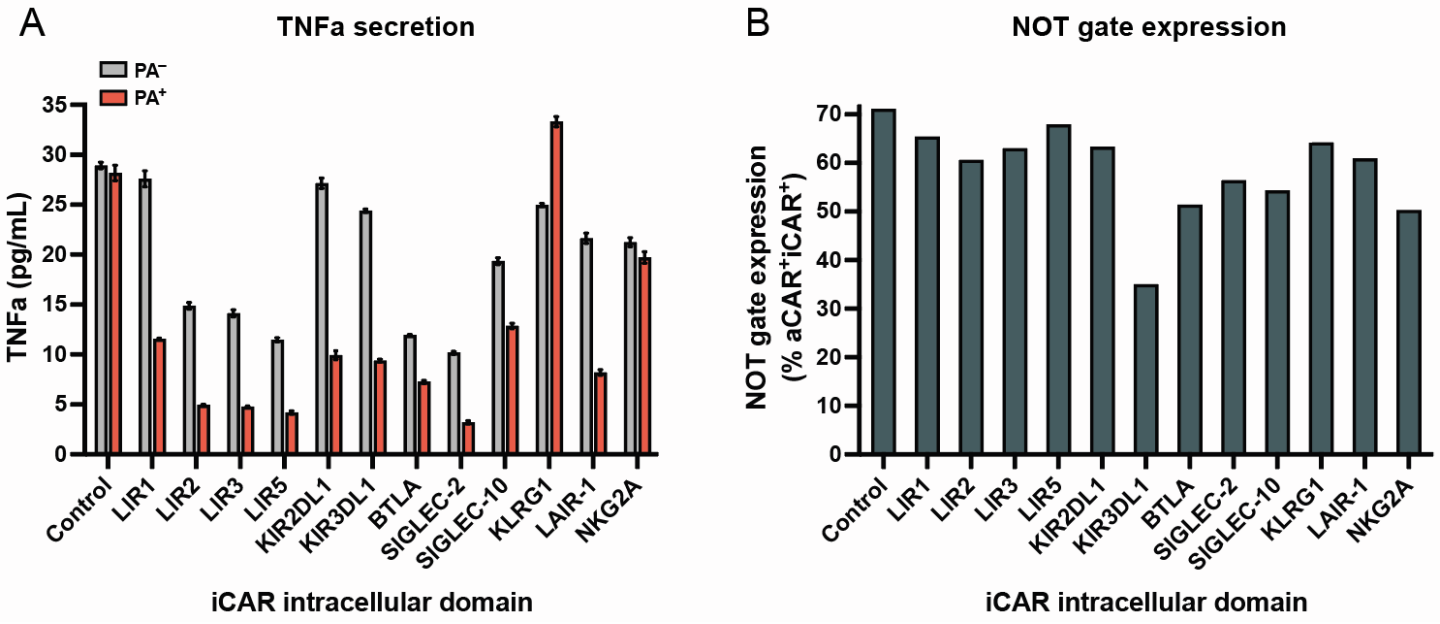

Figure S3. NOT gate screen additional results. A. NK cell secretion of TNFa corresponding to Figure 3B, confirming that LIR1 (group second from left) is a high performing iCAR ICD, characterized by its reduction in off-tumor response while maintaining a high on-tumor response relative to control (leftmost group), as compared to other candidates. B. Expression analysis shows that outcome of iCAR screening in Figure 3B was not solely due to differences in NOT gate expression levels in NK cells. Many candidate iCARs had similar or higher NOT gate expression than LIR1 but performed worse.

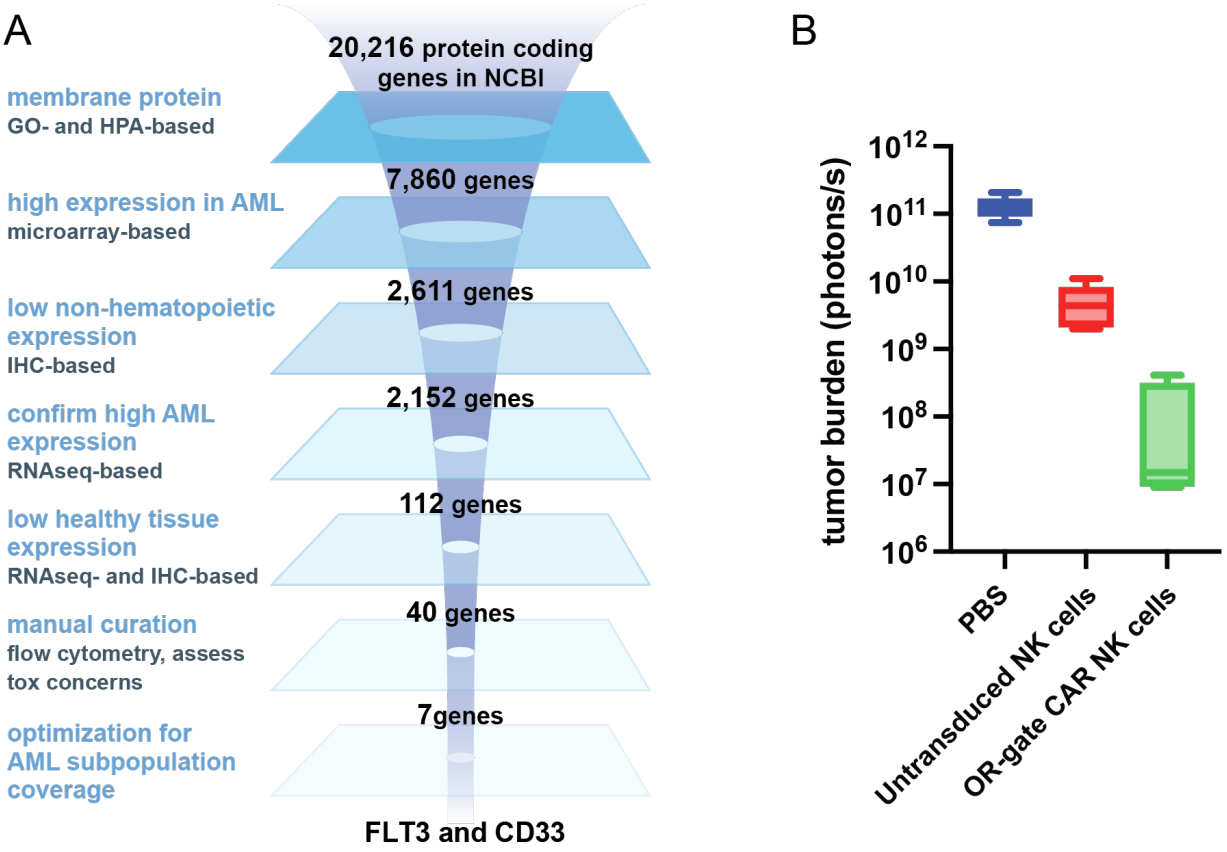

Figure S4. FLT3 OR CD33 gate design and validation. A. Discovery of FLT3 and CD33 targets using an analogous bioinformatic framework to that shown Figure 2B. B. Quantification of bioluminescence imaging shown in Figure 4E. Box shows median of at least 4 mice and the interquartile range, and whiskers show extent of data. Untransduced NK cells partially clear tumor cells but OR-gate CAR-NK cells demonstrated additional killing activity.

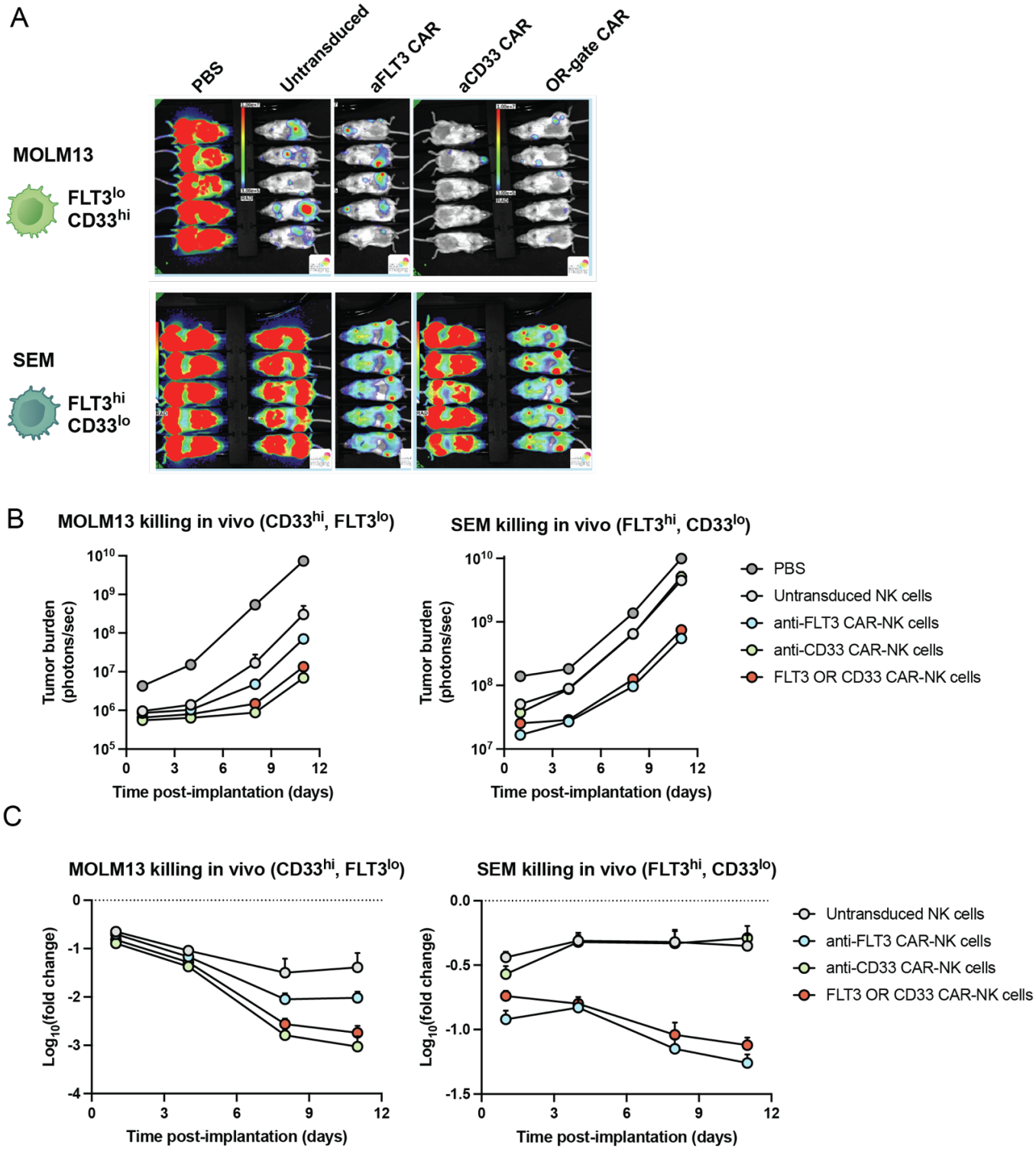

Figure S5. Bioluminescence imaging (BLI) of an in vivo OR gate challenge model corresponding to the experiment shown in Figure 4G. A. Raw images corresponding to the data in Figure 4H. B. Quantified BLI data over time for MOLM13 (left) and SEM (right) models, comparing FLT3 OR CD33 gate-CAR (red) to mono CARs (CD33, green; FLT3, blue) and controls (PBS, dark gray; Untransduced NK cells, light gray). CAR activity delays the increase in tumor burden in an antigen-dependent manner. C. Transformation of data in (B) by $\log_{10}$ fold change relative to the PBS control clarifies differences in CAR performance relative to controls, as shown in Figure 4H. OR gate CAR-NK cells perform similarly to each mono-CAR in its respective “specialized” cancer type (no significant difference by ANOVA). In this figure, values represent the mean of at least 5 mice and error bars represent ± S.E.M, which in some cases was smaller than the size of the marker.

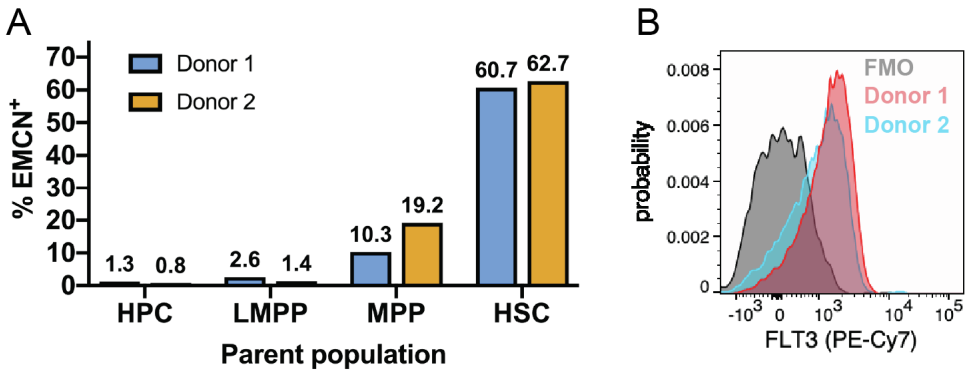

Figure S6. TAA and PA expression on primary human HSCs. A. EMCN expression on various hematopoietic stem and progenitor cell (HSPC) subpopulations in CD34-enriched primary human bone marrow cells, including hematopoietic progenitor cells (HPC), lympho-myeloid primed progenitor cells (LMPPs), multipotent progenitor cells (MPPs), in addition to HSCs, which exhibited over 60% EMCN expression across two representative donors (blue and orange). B. FLT3 expression on HSCs for each representative donor (red and blue) versus a fluorescence-minus-one (FMO) control of Donor 1 (gray). FMO control: anti-FLT3 staining antibody was omitted from a panel that was otherwise the same as the donor samples.

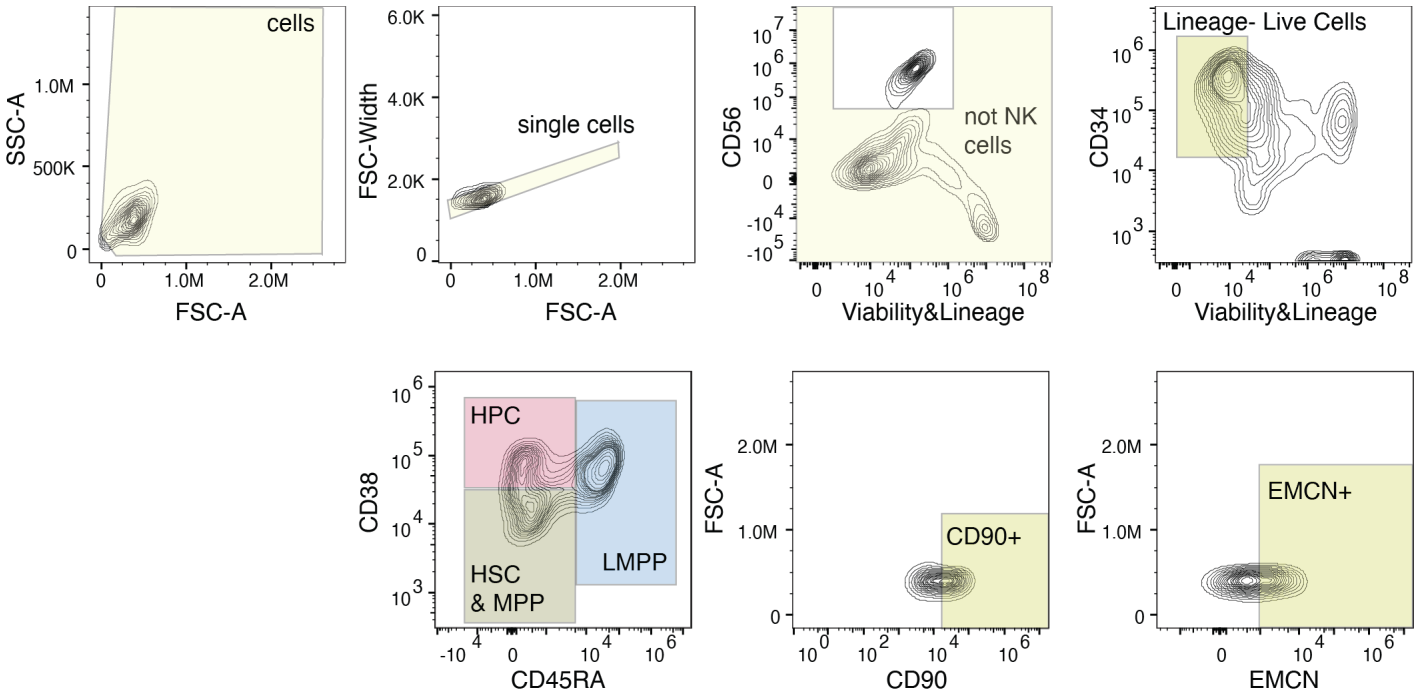

Figure S7. Gating strategy to count the number of live remaining EMCN$^+$ HSCs after killing assay shown in Figure 5E. From left to right and top to bottom, progressive gates on (1) cell size parameters, (2) single cells, (3) CD56-negative cells (i.e., not NK cells), (4) live CD34$^+$ undifferentiated cells, (5) CD45RA$^-$CD38$^-$ cells (i.e., HSCs and MPPs; brown gate; other gates are shown for illustrative purposes), (6) CD90$^+$ cells (i.e., HSCs), and (7) EMCN$^+$ HSCs. Gates for CD90 and EMCN were set using FMO controls. Representative example after 20 hr co-culture with untransduced NK cells is shown. During this period, expression of EMCN decreases slightly due to the innate tendency of primary HSCs to differentiate rapidly in culture.

A

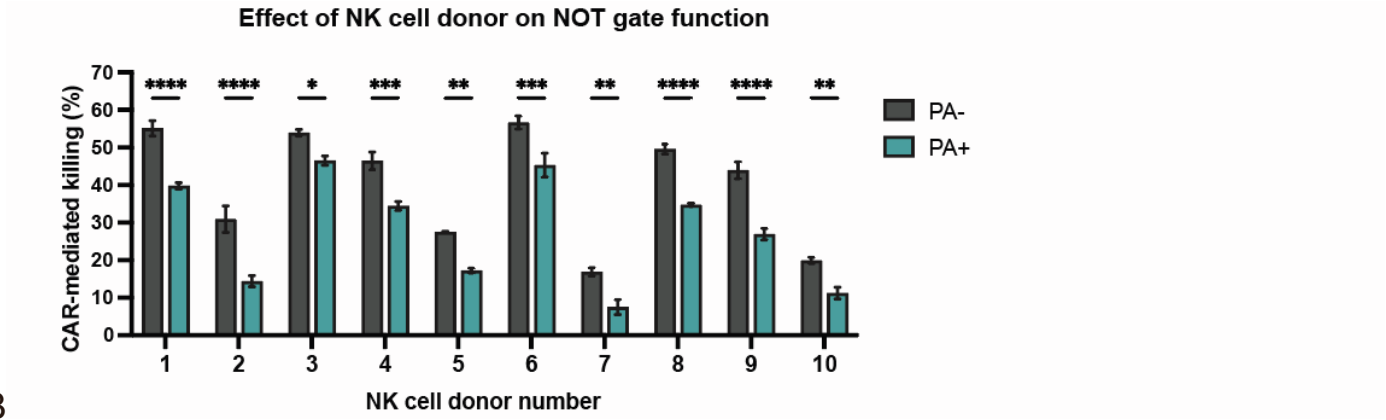

B

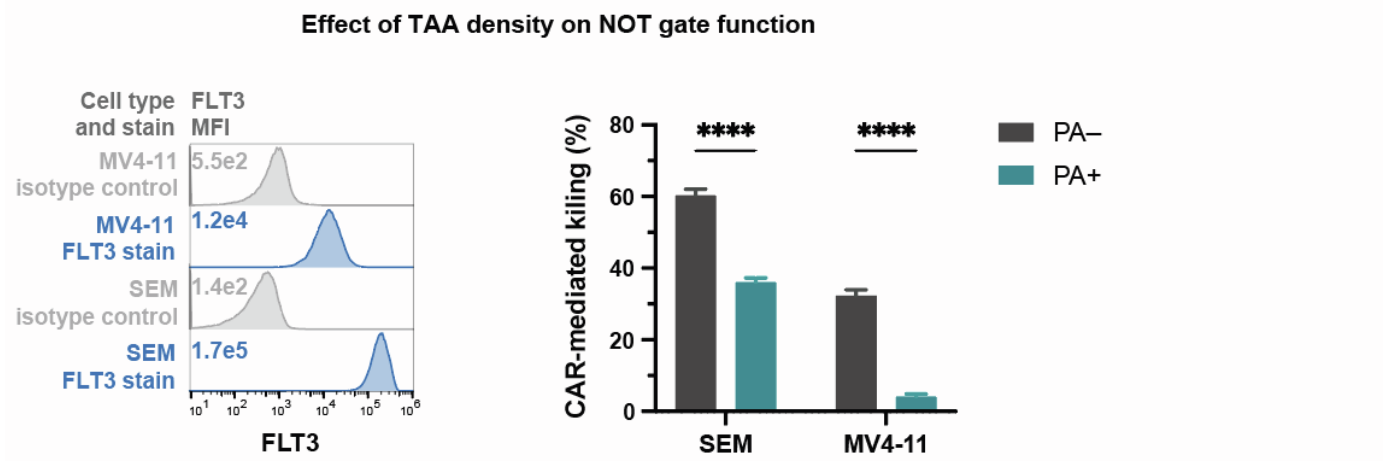

C

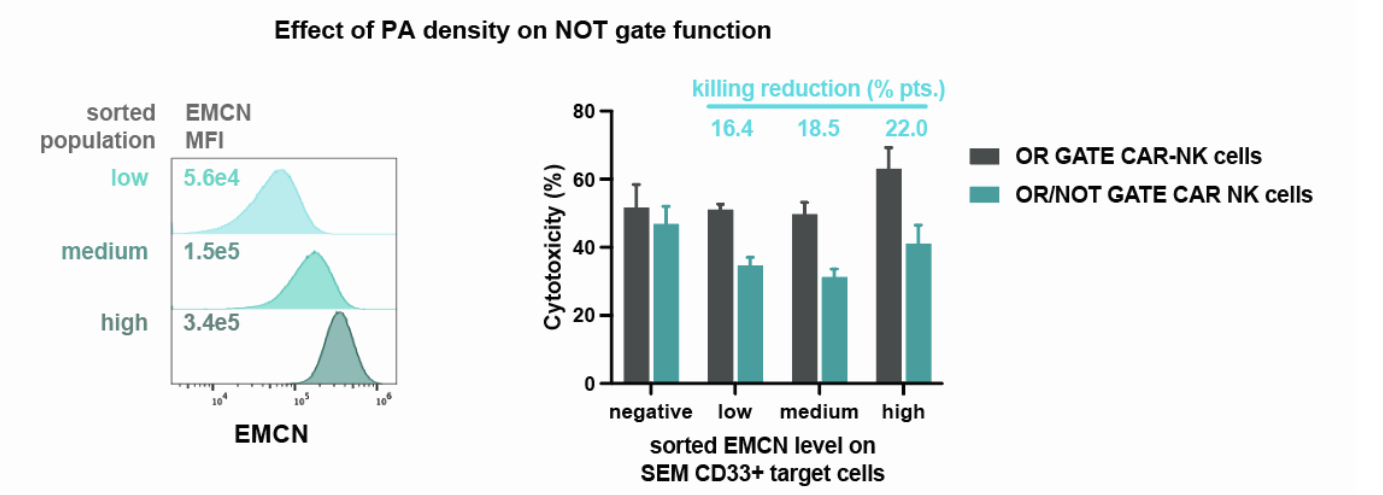

Figure S8. Robustness of three-input OR-NOT gate gene circuit shown in Figure 5B. A. OR-NOT gate CAR-NK cells exhibit functional killing and NOT gate behavior when derived from a large range of NK cell donors. Despite some expected variation in cytotoxicity from donor to donor, effector cells generated from 10 different healthy donors (of 10 tested) confirm CAR-mediated killing of on-target (PA-, gray) cells and statistically significant reduction in killing of off-target (PA+, teal) cells, demonstrating that NOT gate function is robust to NK cell donor. B. OR-NOT gate CAR-NK cells still exhibit NOT gate behavior at lower levels of target TAA expression, although CAR-mediated killing is reduced. Left: FLT3 expression on MV4-11 is an order of magnitude lower than in SEM cells. Right: On- and off-target killing of SEM (left) or MV4-11 (right) cells, expressing EMCN (PA+, teal) or not (PA-, gray), by OR-NOT gate CAR NK cells. The observed lower killing of MV4-11 cells was expected based on the lower FLT3 expression of this cell line, but NOT gate function was nevertheless highly significant, demonstrating the robustness of the circuit to different TAA expression levels. (Figure legend continued on next page)

Figure S8 (continued from previous page) C. OR-NOT gate CAR-NK cells exhibit NOT gate behavior at lower levels of target PA expression, although effect size is reduced. Left: SEM EMCN+ cell line was sorted into three subpopulations, producing three derivative cell lines with different expression levels of EMCN. Right: Killing of sorted EMCN cell lines by either OR gate CAR-NK cells lacking a NOT gate (gray) or the full tricistronic OR-NOT gate CAR-NK cells (teal). NOT gate function was observed at all PA levels, though higher expression levels of EMCN elicited a higher difference in killing. Note that the impact of comparatively “high” or “low” PA levels depend on the cell type. Importantly, Figure 5 shows that endogenous expression levels of EMCN on HSCs are sufficient to elicit a significant protective response. In this figure, values represent the mean of at 3 technical replicates and error bars represent ± S.E.M. Significance was tested using Welch’s test (*$p<0.05$, **$p<0.01$, ***$p<0.005$, ****$p<0.001$).

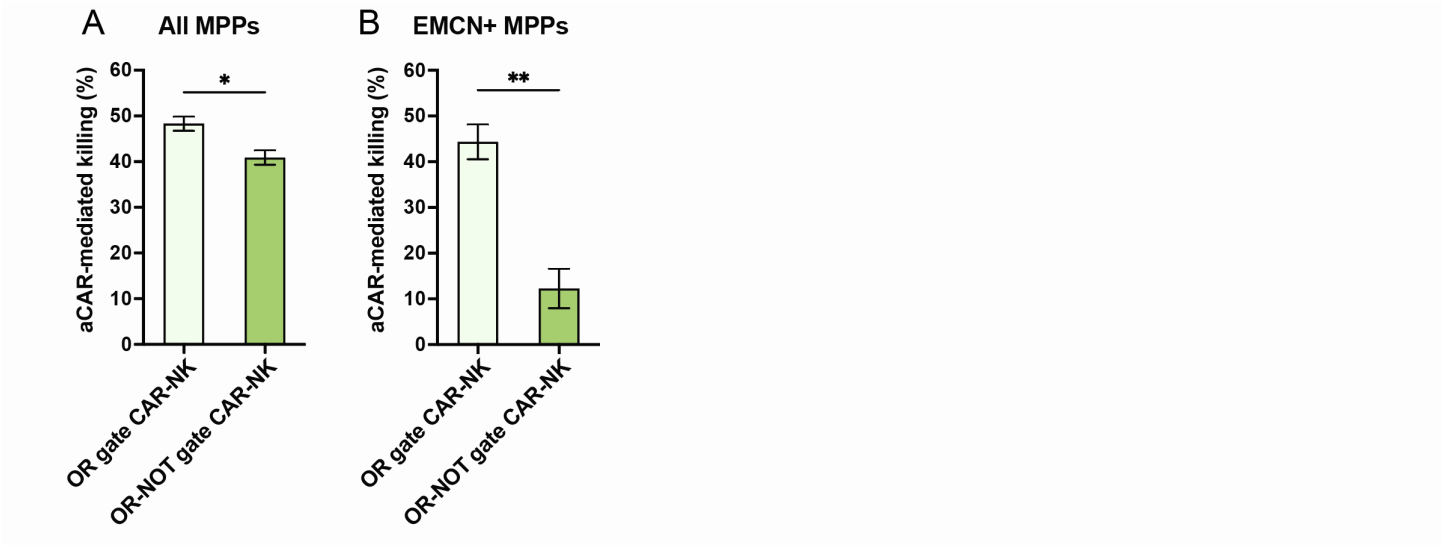

Figure S9. OR-NOT gate CAR-NK cells protect multipotent progenitor cells (MPPs) from OR gate CAR-mediated toxicity. As in Figure 5E, CD34+ bone marrow isolates, containing HSCs, MPPs and other cells, were co-cultured with either OR gate CAR-NK cells lacking a NOT gate (light green) or NK cells expressing the full OR-NOT gate circuit shown in Figure 5B. Subsequently, MPPs were identified by flow cytometry following the gating strategy shown in Figure S7 in order to calculate killing of this subpopulation specifically. A. Considering all MPPs as targets, OR-NOT gate CAR-NK cells exhibit reduced killing compared to the OR gate CAR-NK cells. B. The NOT gate-mediated protection from toxicity was more pronounced when specifically considering EMCN+ MPPs. In this figure, values represent the mean of at 3 technical replicates and error bars represent ± S.E.M. Significance was tested using Welch's test (*$p<0.05$, **$p<0.01$).

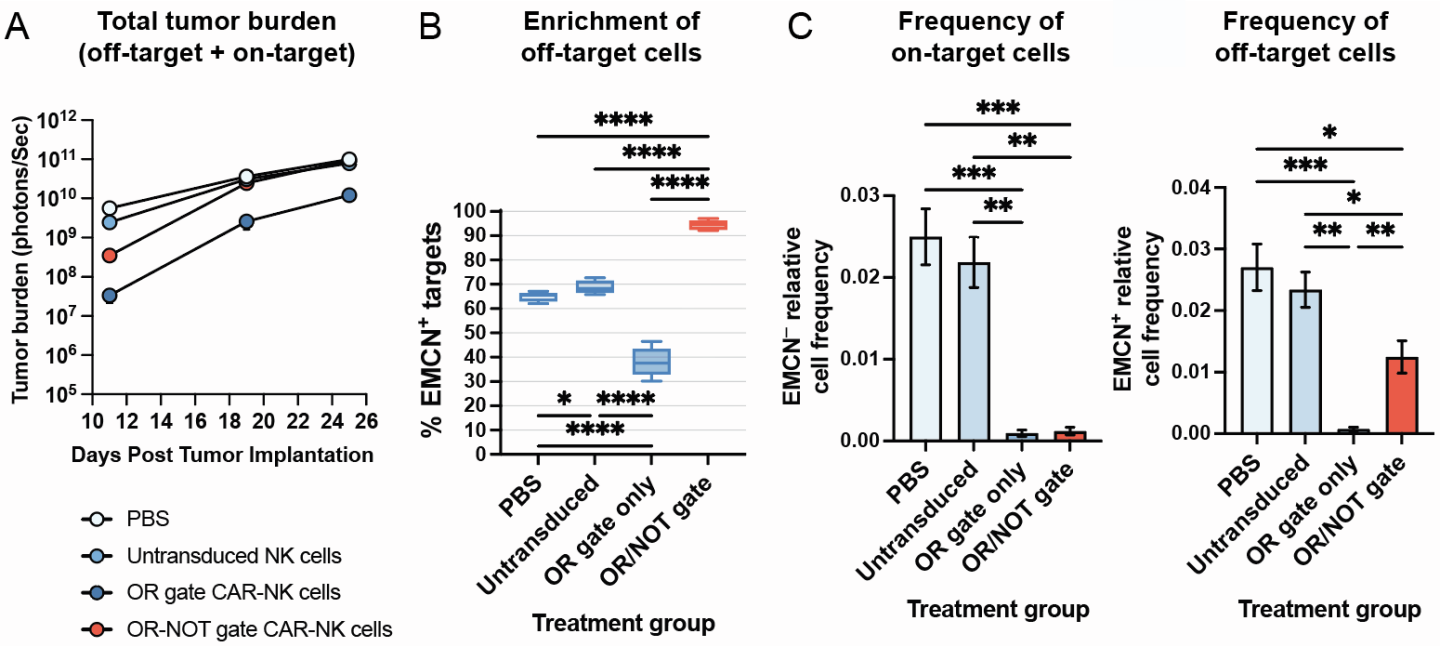

Figure S10. OR-NOT gate CAR-NK cell in vivo validation. A. Quantified whole mouse tumor bioluminescence imaging intensity corresponding to Figure 6. This value reflects the sum of all tumor cells, including both EMCN$^-$ and EMCN$^+$ subpopulations. Values represent the mean of at least 5 mice and error bars represent ± S.E.M. Note that, in some instances, error bars were smaller than the marker size. B. Percent of target cells that express EMCN. Same as Figure 6C but at day 27 post tumor implantation, showing NOT gate effect at this later time point. Although some drift was observed in control treatments (shades of blue) relative to the initial 50% baseline (possible due to compounding of small differences in antigen expression or growth rate), the OR-NOT gate (red) resulted in significant protection of EMCN$^+$ target cells with respect to all controls, enriching them to >90% positivity. Boxes represent interquartile range of at least 5 mice with line at median, and whiskers represent range of data. C. Frequency of the indicated target cell type as a percentage of all CD45$^+$ cells. Same as Figure 6D, but at day 20 post tumor implantation, confirming NOT gate effect at this earlier time point, specifically in the case of OR-NOT gate CAR-NK cell treatment. Values represent the mean of at least 5 mice and error bars represent ± S.E.M. In this figure, statistical significance was determined using ANOVA (*p<0.05, **p<0.01, ***p<0.005, ****p<0.001).